SYNAPSE 50:130–136 (2003)

Effects of Endogenous Agonists, Glycine and D-Serine, on In Vivo Specific Binding of [^{11}C]L-703,717, a PET Radioligand for the Glycine-Binding Site of NMDA Receptors

TERUSHI HARADAHIRA,[1,6]* TAKASHI OKAUCHI,[2] JUN MAEDA,[2] MING-RONG ZHANG,[3] TORU NISHIKAWA,[4] RYOUICHI KONNO,[5] KAZUTOSHI SUZUKI,[1] AND TETSUYA SUHARA[2,6]

[1]*Department of Medical Imaging, National Institute of Radiological Sciences, Inage-ku, Chiba 263-8555, Japan*
[2]*Brain Imaging Project, National Institute of Radiological Sciences, Inage-ku, Chiba 263-8555, Japan*
[3]*SHI Accelerator Service, Shinagawa-ku, Tokyo 141-8686, Japan*
[4]*Department of Psychiatry and Behavioral Sciences, Tokyo Medical and Dental University, School of Medicine, Bunkyo-ku, Tokyo 113-8519, Japan*
[5]*Department of Microbiology, Dokkyo University, School of Medicine, Kitakobayashi, Mibu, Tochigi 321-0293, Japan*
[6]*CREST, Japan Science and Technology Corporation, Kawaguchi 332-0012, Saitama, Japan*

KEY WORDS D-serine; glycine; NMDA receptor; glycine binding site; L-703,717; PET

ABSTRACT A positron-emitter (carbon-11) labeled antagonist for the glycine-binding site of NMDA receptors, [^{11}C]L-703,717, has a unique in vivo binding characteristic, in which it preferentially binds to cerebellar-specific NMDA receptors consisting of a GluRε3 subunit and eventually accumulates in rodent cerebellum under in vivo conditions, but not under in vitro conditions. In order to understand the in vivo-specific site and subunit localization of this radioligand, we examined the effect of the endogenous glycine site agonists, glycine and D-serine, on in vivo [^{11}C]L-703,717 binding. An increase in extracellular glycine concentration by treatment with a glycine transporter 1 (GlyT1)-selective inhibitor, NFPS ethyl ester, significantly decreased the cerebellar localization of [^{11}C]L-703,717 in rats. D-serine is known to be concentrated in mammalian forebrain regions. The lack of D-serine detection in the cerebellum may be due to the fact that it has the highest enzymatic activity of D-amino acid oxidase (DAO). It was found that the cerebellar localization of [^{11}C]L-703,717 is greatly diminished in mutant mice lacking DAO, in which D-serine content in the cerebellum is drastically increased from a nondetectable level in normal mice. These studies indicate that [^{11}C]L-703,717 is susceptible to inhibition by glycine site agonists in its in vivo binding, and suggest that regional differences in inhibitions by endogenous agonists may be a crucial factor in the site- and subunit-specific binding of this glycine-site antagonist. **Synapse 50:130–136, 2003.**

INTRODUCTION

With the recent identification of a link between *N*-methyl-D-aspartate (NMDA) receptor activation, neurodegeneration, and cell death, there has been increased interest in developing radioligands for use in in vivo NMDA receptor imaging by positron emission tomography (PET). Functional NMDA receptors in adult CNS are formed by a combination of at least one GluRζ1 subunit and one or more GluRε (ε1–ε4) subunits (for review, see Mori and Mishina, 1995). GluRζ1 subunit is distributed ubiquitously in the brain, whereas the four GluRε subunits exhibit distinct distributions in the brain. GluRε1 subunit is expressed in all brain regions, while the GluRε2, GluRε3, and GluRε4 subunits are localized in forebrain regions: cer-

*Correspondence to: Terushi Haradahira, Department of Medical Imaging, National Institute of Radiological Sciences, 4-9-1 Anagawa, Inage-ku, Chiba 263-8555, Japan. E-mail: terushi@nirs.go.jp

Received 11 November 2002; Accepted 12 June 2003

DOI 10.1002/syn.10254

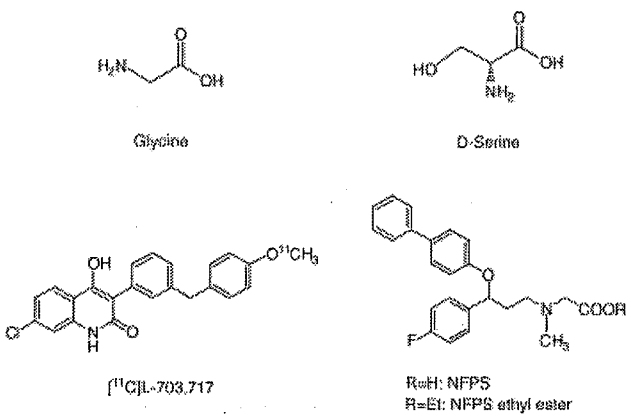

Fig. 1. The chemical structures of glycine, D-serine, [^{11}C]L-703,717, NFPS, and its ethyl ester.

ebellum and diencephalic/lower brainstem, respectively. We recently developed a PET radioligand for the glycine binding site of NMDA receptors, [^{11}C]L-703,717 (Fig. 1), and found that this radioligand only localizes in the cerebellar NMDA receptors consisting of the GluRε3 subunit under in vivo conditions, but not under in vitro conditions (Haradahira et al., 2002). This was the first demonstration of the in vivo binding of a glycine-site antagonist to a specific subunit of NMDA receptors, and therefore [^{11}C]L-703,717 may be a useful tool to investigate the role of cerebellar NMDA receptor subtype in physiological and pathophysiological processes by PET.

Various endogenous ligands acting at NMDA receptors, such as amino acids, polyamines, and divalent/monovalent cations, are abundant, existing in micromolar to millimolar quantities in the CNS (for review, see Danysz and Parsons, 1998; Dingledine et al., 1999). It is therefore probable that such high levels of endogenous ligands directly or indirectly modulate radioligand binding in vivo, especially in the case where the radioligand would share the binding site with such endogenous ligands. Furthermore, such modulations might differ by regions or by other subunit compositions. Glycine and D-serine are amino acids acting as co-agonists with glutamate at the site of NMDA receptors and exist in micromolar quantities with characteristic regional brain distributions. Glycine is distributed throughout the brain, but to a higher degree in rat brain stem regions and spinal cord (Hashimoto et al., 1993b; Schell et al., 1997). D-Serine is localized only in the mammalian forebrain regions and, very interestingly, is almost free in the cerebellum due to the highest activity of D-amino acid oxidase (DAO) in the cerebellum (Hashimoto et al., 1993a,b, 1995; Schell et al., 1995, 1997; Weimar and Neims, 1977). Such regional variations in agonist concentrations might be involved in the site determination and subunit-preferential binding of [^{11}C]L-703,717. In order to confirm this hypothesis, we examined whether or not the in vivo distribution of [^{11}C]L-703,717 in rodents is affected by changes of agonist concentrations in the brain. In the CNS, the glycine transporter GlyT1 has been identified (for review, see Malandro and Kilberg, 1996; Palacín et al., 1998). GlyT1 is coupled to NMDA receptors and glycine is actively taken up through this transporter by cells. We employed a GlyT1-selective inhibitor, *N*[3-(4′-fluorophenyl)-3-(4′-phenyphenoxy)propyl]sarcosine (NFPS, Fig. 1) (Aubrey and Vandenberg, 2001; Bergeron et al., 1998), to increase the extracellular concentrations of endogenous glycine. Due to a low brain uptake of NFPS, confirmed by our in vivo distribution studies using carbon-11-labeled NFPS ([^{11}C]NFPS) (Zhang et al., 2000), an ethyl ester of NFPS was used for the blocking of rat GlyT1 activity in vivo. [^{11}C]NFPS ethyl ester showed a 3-fold increase in brain uptake compared to [^{11}C]NFPS followed by a rapid bioconversion into free acid in rodents and monkey (Zhang et al., 2000). In order to increase the extracellular D-serine concentration, we employed mutant mice lacking DAO activity, in which it was reported that D-serine content in the cerebellum is drastically increased from a nondetectable level in normal mice (Hashimoto et al., 1993a).

MATERIALS AND METHODS

NFPS ethyl ester was synthesized by the following sequence of reactions: *N*-alkylation of sarcosine ethyl ester with 3-chloro-4′-fluoropropiophenon, reduction of the carbonyl group with sodium borohydride, and dehydration with 2-phenylphenol using triphenylphosphine and diethyl azodicarboxylate (Manhas et al., 1975). The chemical structure of the product was identified by ^{1}H-NMR, mass spectrum, and elemental analysis to be NFPS ethyl ester. Normal male (ddY/DAO$^+$) mice weighing 56–62 g and DAO-deficient (ddY/DAO$^-$) mice weighing 40–52 g were used (Konno et al., 1983). [^{11}C]L-703,717 was synthesized as described in the literature (Haradahira and Suzuki, 1999). All animal experiments were carried out according to the recommendations of the Committee for the Care and Use of Laboratory Animals, National Institute of Radiological Sciences, Japan.

Microdialysis

Male Sprague-Dawley rats weighing 180–200 g were housed three or four per cage at a constant room temperature (25°C) under a 12-h light-dark cycle (lights: 7:00–19:00) for 2–4 weeks. The rats were anesthetized with sodium pentobarbital (60 mg/kg, i.p.) and then placed in a stereotactic apparatus. A guide cannula of 8-mm length (Eicom Corp., Japan) was surgically implanted into the prefrontal cortex (coordinates A +2.5 mm, L +0.6 mm, V –3.0 mm from bregma) and cerebellum (coordinates A –11.3 mm, L +2.5 mm, V –5.0 mm from bregma) with reference to a brain atlas. The

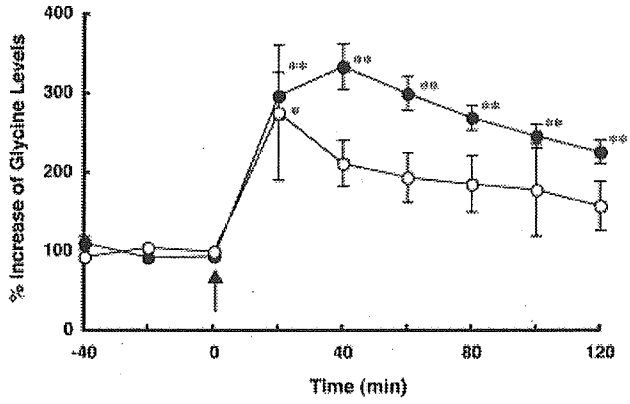

Fig. 2. Effect of NFPS ethyl ester on basal extracellular concentrations of glycine in rat prefrontal cortex (closed circles) and cerebellum (open circles). Arrow indicates the time of injection of NFPS ethyl ester (10 mg/kg, i.v.). The results are mean ± SEM of 3–4 animals and expressed as percentages of basal levels. $^{*}P < 0.05$ vs. basal level in the cerebellum, $^{**}P < 0.01$ vs. basal level in the prefrontal cortex.

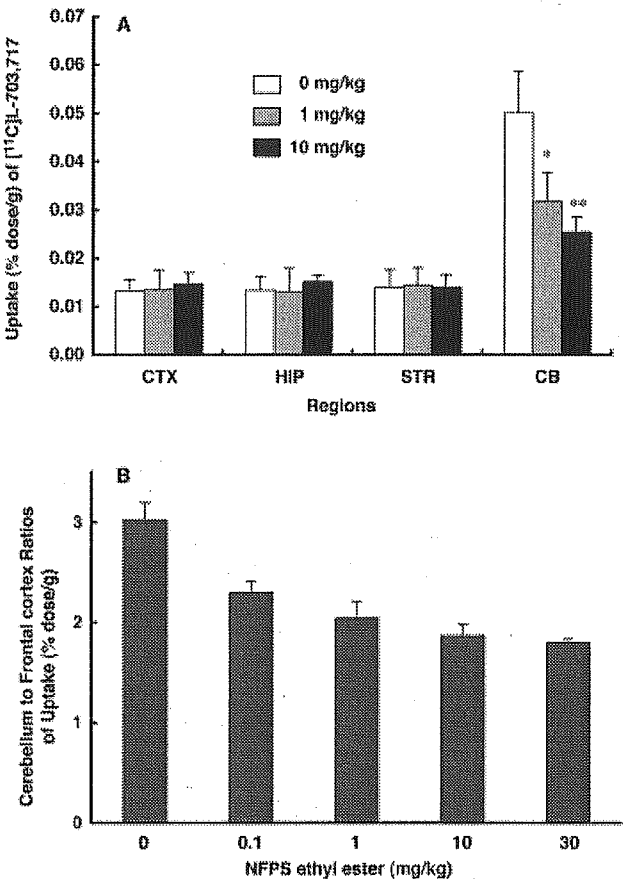

Fig. 3. Effect of endogenous glycine on in vivo brain distribution of [^{11}C]L-703,717 in rats. **A:** The regional brain distribution of [^{11}]L-703,717 in control and NFPS ethyl ester-treated rats. NFPS ethyl ester was injected i.v. at 10 min before the [^{11}C]L-703,717 injection and the rats were killed at 20 min after the [^{11}C]L-703,717 injection. The results are mean ± SD of three rats and expressed as % dose/g of tissue. CTX, cerebral cortex; HIP, hippocampus; STR, striatum; CB, cerebellum. $^{*}P < 0.01$ (NFPS ethyl ester, 0 mg/kg vs. 1 mg/kg in CB), $^{**}P < 0.01$ (NFPS ethyl ester, 0 mg/kg vs. 10 mg/kg in CB). **B:** The uptake ratios of cerebellum to frontal cortex after the treatments of NFPS ethyl ester (0–30 mg/kg).

rats were allowed to recover for at least 2 days before the infusion experiments.

On the day of infusion a microdialysis probe (membrane length 3.0 mm, Eicom) was inserted via the guide cannula under light anesthesia with diethyl ether and the cannula was fixed with a screw. The probe was perfused with 2.0 μl/min of Ringer's solution (147 mM Na^+, 4 mM K^+, 2.3 mM Ca^{2+}, 155.6 mM Cl^-). The outflow from the prefrontal cortex was collected with a fraction collector and sampling was started 3 h after the start of infusion at 20-min intervals. NFPS ethyl ester (10 mg/kg, i.v.) was administered via a tail vein to evaluate the effect on basal glycine release. The glycine in the dialysates was automatically mixed with 4 mM *o*-phthaldialdehyde and 2-mercaptoethanol in 0.1 M potassium carbonate-HCl buffer (pH 9.5) at a ratio of 3:1 for 2.5 min at 5°C. Then the mixture was injected into an HPLC-fluorometric detector (excitation wave length 340 nm, emission wave length 445 nm) system with a reversed-phase column (EICOMPAK SC-50ODS, ϕ 3.0 × 150 mm). We used 0.1 M phosphate buffer (pH 6.0) containing EDTA2Na (5 mg/l) and methanol (30% of total volume) as a mobile phase at a flow rate of 1.0 ml/min. The increases in glycine concentrations in prefrontal cortex and cerebellum after the pretreatments of NFPS ethyl ester were observed and are summarized in Figure 2.

Brain distribution in NFPS-treated rats

Male Sprague-Dawley rats (270–280 g) were pretreated with NFPS ethyl ester (0.1–30 mg/kg, i.v.) at 10 min before radioligand injection. The NFPS-treated rats were injected i.v. with [^{11}C]L-703,717 (0.3–0.5 ml, ~17 MBq) containing warfarine (55 mg/kg), which was used to prevent plasma protein binding of the radioligand (Haradahira et al., 2000). The rats were killed under ether anesthesia at 20 min after the radioligand injection, the brains were removed and dissected into cerebral cortex, hippocampus, striatum, and cerebellum. Radioactivity in each sample was measured with a Packard γ-counter and corrected for decay. The results were expressed as the percent administered dose per gram of tissue (% dose/g) (Fig. 3).

Brain distribution in DAO-deficient mice

The combined solution of [^{11}C]L-703,717 (0.2 ml, ~55 MBq/ml) and warfarine (55 mg/kg) was injected via a tail vein into ddY/DAO^+ (n = 5) or into ddY/DAO^- mice (n = 6). The animals were killed at 30 min after the injection by decapitation and brains were rapidly removed. The brains were further dissected into cerebral cortex, hippocampus, striatum, and cerebellum. Radioactivity in each sample was measured with a Packard γ-counter and corrected for decay. Due to the difference

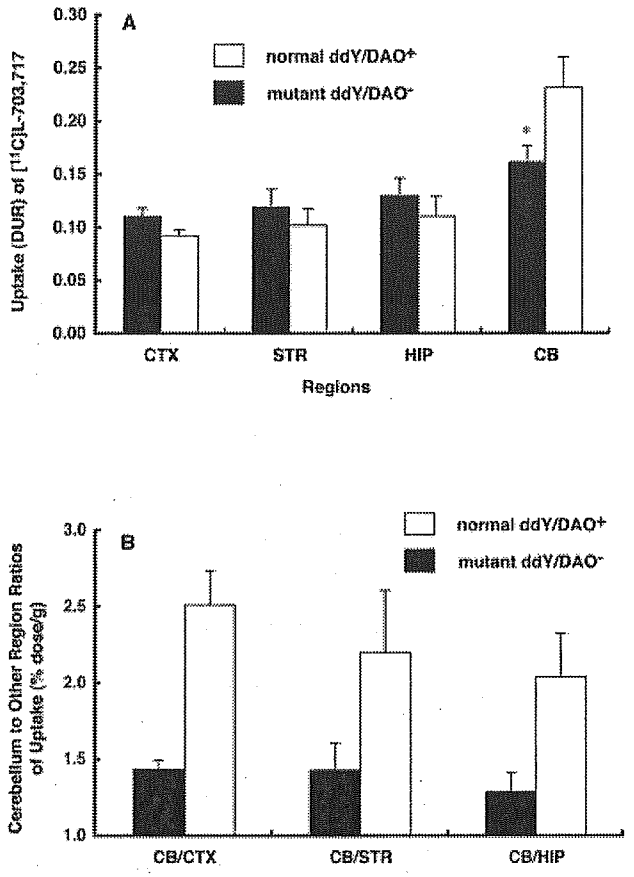

Fig. 4. Effect of endogenous D-serine on in vivo brain distribution of [^{11}C]L-703,717 in mice. **A:** The regional brain distributions of [^{11}C]L-703,717 in normal ddY/DAO$^+$ and mutant ddY/DAO$^-$ mice. [^{11}C]L-703,717 was injected intravenously via a tail vein and the mice were killed at 30 min after the [^{11}C]L-703,717 injection. The results are mean ± SD of 5-6 mice and expressed as differential uptake ratio (DUR). CTX, cerebral cortex; STR, striatum; HIP, hippocampus; CB, cerebellum. *$P < 0.01$ (DAO$^+$ vs. DAO$^-$ in CB). **B:** The uptake ratios of cerebellum to other regions in normal ddY/DAO$^+$ and mutant ddY/DAO$^-$ mice. The results are expressed as the radioactivity (% dose/g) ratios of the cerebellum to cortex (CB/CTX), cerebellum to striatum (CB/STR), and cerebellum to hippocampus (CB/HIP).

in body weight between normal and DAO-deficient mice, the result of each sample was expressed as differential uptake ratio (DUR) = (% dose/g) × body weight (g)/100 (Fig. 4A) to normalize the mouse body weight. The radioactivity ratios of cerebellum to other regions were calculated as the ratios of the corresponding % dose/g (Fig. 4B).

Ex vivo autoradiography

The combined solution of [^{11}C]L-703,717 (110 MBg/0.5 ml) and warfarine (50 mg/kg) was injected intravenously via a tail vein to ddY/DAO$^+$ or ddY/DAO$^-$ mice. After 30 min, the mice were killed under ether anesthesia and the brain was quickly removed, frozen in dry ice, and cut into sagittal sections (50 μm) on a cryostat microtome (MICROM HM560, Carl Zeiss, Germany). These sections were thaw-mounted on a microcover glass (Matsunami Glass Ind., Osaka, Japan), dried on a hot plate (50–60°C), and exposed to imaging plates for 60 min (BAS-SR 127, Fuji Photo Film). The distribution of radioactivity accumulated in the imaging plates was assessed by FUJIX BAS 3000 bioimaging analyzer and visualized as shown in Figure 5.

Statistical analyses

Analyses of data were performed using a repeated measures ANOVA with either a multiple comparison (Tukey's WSD) or a simple main effect test where appropriate for post-hoc test.

RESULTS

The microdialysis studies clarified that intravenous injection of NFPS ethyl ester (10 mg/kg) rapidly increases the extracellular concentrations of glycine up to ~300% of baseline concentrations (1.1 μM for prefrontal cortex, 4.4 μM for cerebellum) in both prefrontal cortex and cerebellum (Fig. 2). Repeated ANOVA showed a significant main effect of the time course of glycine release in the prefrontal cortex ($F_{8/16} = 35.98$, $P < 0.01$) and in the cerebellum ($F_{8/24} = 2.57$, $P < 0.05$). The post-hoc (multiple comparison) test revealed significant increases in the glycine concentrations at the all time points after the drug treatment in the prefrontal cortex and at 20 min after the drug treatment in the cerebellum. No significant changes of concentrations were observed in other amino acids including L-glutamate, D,L-serine, and D,L-aspartate. One notable finding was that the return of the glycine concentration to the baseline level was faster in the cerebellum than in the prefrontal cortex. On the basis of these microdialysis studies, NFPS ethyl ester was injected into rats at 10 min before [^{11}C]L-703,717 injection and the rats were killed at 20 min after [^{11}C]L-703,717 injection (at 30 min after the NFPS-treatment), during which time the extracellular glycine concentrations can be expected to be maintained at their highest level in the brains of NFPS-treated rats. The regional brain uptakes of [^{11}C]L-703,717 after the treatment with NFPS ethyl ester are summarized in Figure 3. The uptake (% dose/g) of [^{11}C]L-703,717 in NFPS-treated rats was significantly reduced in the cerebellum, but not, because of nonspecific bindings (Haradahira et al., 2000), in the other regions (cerebral cortex, hippocampus, and striatum) (Fig. 3A). Repeated ANOVA on the dose of NFPS ethyl ester for the four brain regions revealed a significant dose × region interaction ($F_{6/18} = 5.50$, $P < 0.01$). The post-hoc test using the simple main effect in each region and subsequent the multiple comparison yielded significant decreases in the cerebellum ($F_{2/24} = 8.07$, $P < 0.01$) in a dose-dependent manner. The uptake ratio of the cerebellum to frontal cortex was reduced in dose-dependent manner as shown in Figure 3B. These results indicate that the increase in extra-

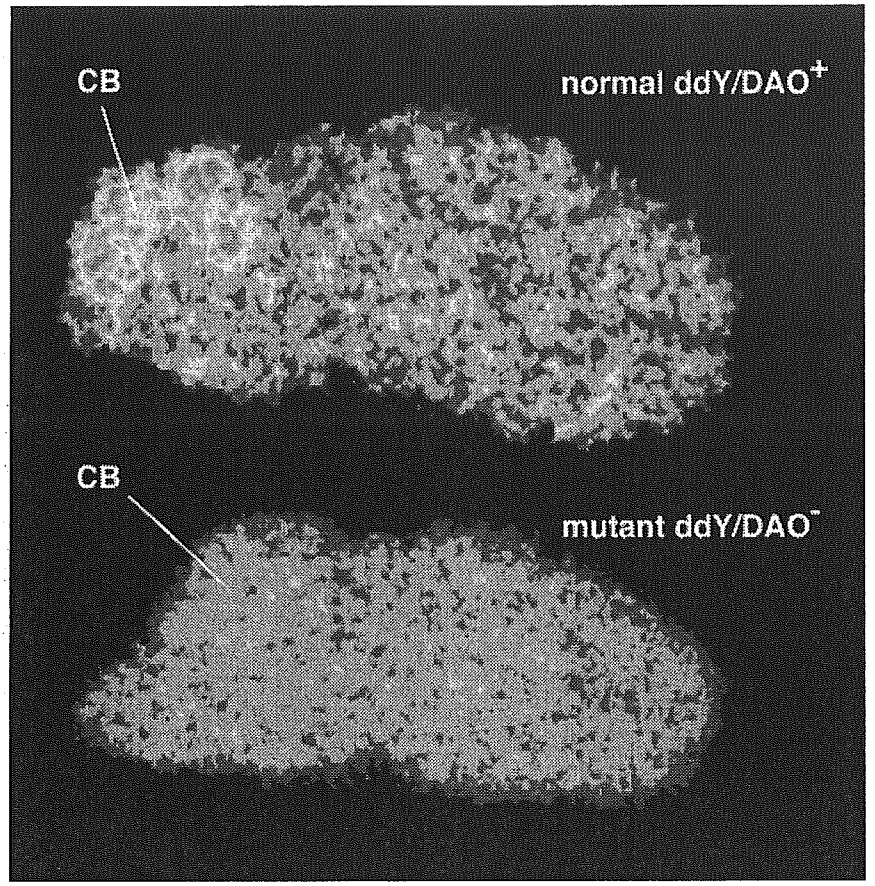

Fig. 5. Ex vivo autoradiographic localizations of [^{11}C]L-703,717 in the brains of normal ddY/DAO$^+$ and mutant ddY/DAO$^-$ mice. The brain slices (50 μm) were obtained at 30 min after the [^{11}C]L-703,717 injection, placed in contact with imaging plates, and the radioactivity distributions on the plates were analyzed and visualized by BAS 1800 bioimaging analyzer.

cellular glycine concentrations results in a decrease in the specific binding of the glycine antagonist, probably due to the competitive inhibitions.

Nishikawa and co-workers reported that the content of D-serine in the serum and cerebellum of mutant ddY/DAO$^-$ mouse is much higher than that of normal ddY/DAO$^+$ mouse (Hashimoto et al., 1993a). Therefore, in order to examine the effect of D-serine concentration on in vivo [^{11}C]L-703,717 brain distributions, we compared the regional brain uptake of [^{11}C]L-703,717 between normal ddY/DAO$^+$ and mutant ddY/DAO$^-$ mice, the results being shown in Figure 4. The high cerebellar localization of the radioligand observed in normal ddY/DAO$^+$ mice was significantly diminished in mutant ddY/DAO$^-$ mice (Fig. 4A). Repeated ANOVA on the mouse strain for the four brain regions showed a significant strain × region interaction ($F_{3/21} = 21.15$, $P < 0.01$), followed by the test of the simple main effect in each region designated a significant difference in the cerebellum. The ratios of radioactivity of the cerebellum to the other regions were 2.0–2.5 for normal ddY/DAO$^+$ mice and 1.3–1.4 for mutant ddY/DAO$^-$ mice (Fig. 4B). Furthermore, ex vivo autoradiographies visually demonstrated a great reduction in the cerebellar [^{11}C]L-703,717 localization in the mutant ddY/DAO$^-$ mouse in contrast to the normal ddY/DAO$^+$ mouse (Fig. 5). These results indicate that, similar to glycine, the increase in D-serine concentration in the cerebellum greatly reduces the specific [^{11}C]L-703,717 binding in the cerebellum.

DISCUSSION

The present studies using mutant ddY/DAO$^-$ mice and NFPS-treated rats have demonstrated that the cerebellar-specific binding of [^{11}C]L-703,717 was strongly inhibited by an increase in agonist concentrations. Therefore, it has been proven that [^{11}C]L-703,717 is susceptible to inhibition by the endogenous amino acids glycine and D-serine in its in vivo binding. These inhibitions would occur in a competitive manner because the glycine antagonist would share the binding site with glycine agonists.

Glycine plays important roles as a neurotransmitter in mammalian CNS through two distinct types of receptors, strychnine-sensitive glycine$_A$ receptors and strychnine-insensitive glycine$_B$ binding sites coupled to NMDA receptors (Danysz and Parsons, 1998). It was previously demonstrated that free D-serine exists predominantly in mammalian brains at exceptionally high content and also acts as an endogenous agonist for glycine$_B$ binding sites (Hashimoto et al., 1993b; Matsui et al., 1995; Schell et al., 1995, 1997). These two amino

acids exist in brains at a similar range of extracellular concentrations but show a discrete and complementary distribution in the CNS. In rodents, glycine distributes throughout the brain, but to a higher degree in the spinal cord and brain stem regions, whereas D-serine is concentrated only in the forebrain regions and is very low in the cerebellum (Danysz and Parsons, 1998; Hashimoto et al., 1993b; Shell et al., 1997).

Reuptake systems for neurotransmitter amino acids into presynaptic nerve endings or neighboring glial cells provide an efficient mechanism for controlling extracellular amino acid contents, by which synaptic action can be terminated (Gadea and López-Colomé, 2001; Malandro and Kilberg, 1996; Palacín et al., 1998). At least two different genes encoding reuptake systems for glycine have been identified and termed GlyT1 and GlyT2, and they are colocalized with glycine$_B$ and glycine$_A$ receptors, respectively. GlyT1 plays a critical role in the control of extracellular glycine concentrations at the NMDA receptors (Supplisson and Bergman, 1997), and recently a novel GlyT1-selective inhibitor, NFPS, was developed (Aubrey and Vandenberg, 2001; Bergeron et al., 1998). We employed the ethyl ester of NFPS to increase the brain extracellular glycine concentrations under in vivo conditions and found that the glycine concentrations are transiently increased to 300% of controls after i.v. injection of NFPS ethyl ester (10 mg/kg) in rats. Recently, Na^+-dependent neutral amino acid transporters (ASCT1 and ASCT2) were cloned and characterized and D-serine exerted significant inhibition on ASCT2, but not ASCT1, despite a low expression of ASCT2 mRNA in the CNS (Utsunomiya-Tate et al., 1996). Furthermore, a novel Na^+-independent neutral amino acid transporter, Asc1, was identified and characterized to exhibit substantial affinity for D-serine in the brain tissue of the mouse (Fukasawa et al., 2000) and human (Nakauchi et al., 2000). Na^+-dependent uptake of [^{3}H]D-serine by synaptosomal P2 fraction has also been demonstrated in the rat neocortex (Yamamoto et al., 2001).

Metabolisms of amino acids in CNS are alternative mechanisms for regulation of their extracellular contents. The glycine cleavage system (GCS) and D-amino acid oxidase (DAO) are known to be major pathways of degradation of glycine and D-serine, respectively, and the regional brain distributions of these enzymes were reported to be inversely correlated with those of their substrates (Daly et al., 1976; Schell et al., 1995). This is especially true for the DAO, as it is confined to the hindbrain, with the highest activity in the cerebellum where the D-serine concentration is the lowest (Schell et al., 1995). It has been reported that the cerebellar D-serine content in the mutant ddY/DAO$^-$ mouse is increased from a nondetectable level to about half of that in the normal rat forebrains, although the D-serine contents in other regions were not significantly altered (Hashimoto et al., 1993a). The extracellular glycine concentrations in the cerebellum and prefrontal cortex of normal mice were determined to be about 4 μM and 1 μM, respectively, by the present microdialyses. Although the glycine content in the cerebellum was 4-fold that in the prefrontal cortex, it has been reported that regional expressions of both GlyT1 and GlyT2, as well as GCS, are relatively high in the rodent cerebellum as compared to the forebrain regions (Daly et al., 1976; Guastella et al., 1992; Jursky and Nelson, 1995; Zafra et al., 1995), suggesting that the glycine concentration in the vicinity of the cerebellar glycine binding sites might be well controlled to be below its extracellular concentrations. The rapid recovery of the glycine level in the cerebellum to the basal level after NFPS-treatment (Fig. 2) may be suggestive of its rapid reuptake and/or degradation in the cerebellum.

These regional variations in glycine and D-serine concentrations may cause a regional difference in the magnitude of NMDA receptor activation and may generate a functional diversity of this receptor subtype in local brains. Furthermore, in terms of radioligand binding, these variations may affect the local brain distribution of the radioligand targeted to the glycine binding sites. Taking into account the present results using mutant ddY/DAO$^-$ mice, in which the cerebellar-specific [^{11}C]L-703,717 binding had almost disappeared by the increase in D-serine content to about half of that in the normal mouse forebrains, it may be reasonable to suppose that the loss of the specific binding of [^{11}C]L-703,717 in rodent forebrain regions is due to the strong inhibition by the highest content of D-serine. Similarly, the specific binding of [^{11}C]L-703,717 to the glycine site in brain stem and spinal cord, regions known to have the highest glycine concentrations, may also be inhibited by glycine. Thus, the PET radioligand [^{11}C]L-703,717 only localizes in rodent cerebellum under in vivo conditions, but not under in vitro conditions.

Major NMDA receptor subunits expressed in mammalian cerebellum are GluRζ1/GluRε1 and GluRζ1/GluRε3 compositions. Very recently, we demonstrated that [^{11}C]L-703,717 predominantly binds to GluRζ1/GluRε3 subunits, but not to GluRζ1/GluRε1 subunits, under in vivo conditions by employing GluRε3 deficient mice (Haradahira et al., 2002). Although some glycine antagonists have been reported to show intrinsic subunit selectivity (Danysz and Parsons, 1998; Honer et al., 1998), this was not the case here because in vitro [^{11}C]L-703,717 binding to rodent brain slices displayed specific bindings to all brain regions in accordance with the magnitude of NMDA receptor expression in brains (Haradahira et al., 2002). It is well known that NMDA receptors have different pharmacological profiles according to the different subunit compositions (for review, see Yamakura and Shimoji, 1999). For example, the affinities of GluRζ1/GluRε3 subunits for L-glutamate and glycine were higher than those of GluRζ1/

GluRε1 subunits. On the other hand, GluRζ1/GluRε1 subunits were more sensitive to Mg^{2+} block of NMDA receptors than GluRζ1/GluRε3 subunits. Therefore, although the regional variations in glycine and D-serine concentrations also appear to be involved in the in vivo-specific subunit binding of [^{11}C]L-703,717, the mechanism for this may be rather complex and the effects of other endogenous modulators acting at NMDA receptors such as glutamate, polyamines, and divalent/monovalent cations should also be examined in order to understand the in vivo-specific subunit binding of [^{11}C]L-703,717.

In conclusion, the present studies indicate that although [^{11}C]L-703,717 binds to all subunits of the NMDA receptors, regional brain differences in [^{11}C]L-703,717 binding might be determined by regional brain differences in endogenous agonist levels. Since the expression of NMDA-receptor subunits in brains is region-specific, regional variations in endogenous agonist concentrations might also reveal preferential [^{11}C]L-703,717 binding to specific subunits. Especially, it should be noted that the lack of D-serine inhibition in the cerebellum may be a crucial factor in the site and/or subunit-specific localization of [^{11}C]L-703,717.

ACKNOWLEDGMENTS

We thank T. Henmi and N. Nengaki for their support in ^{11}C-methylation. We thank Dr. A. Niwa, Dokkyo University, for helpful advice.

REFERENCES

Aubrey KR, Vandenberg RJ. 2001. *N*[3-(4'-fluorophenyl)-3-(4'-phenylphenoxy) propyl]sarcosine (NFPS) is a selective persistent inhibitor of glycine transport. Br J Pharmacol 134:1429–1436.

Bergeron R, Meyer TM, Coyle JT, Greene RW. 1998. Modulation of *N*-methyl-D-aspartate receptor function by glycine transport. Proc Natl Acad Sci USA 95:15730–15734.

Daly EC, Nadi NS, Aprison MH. 1976. Regional distribution and properties of the glycine cleavage system within the central nervous system of the rat: evidence for an endogenous inhibitor during in vitro assay. J Neurochem 26:179–185.

Danysz W, Parsons CG. 1998. Glycine and N-methyl-D-aspartate receptors: physiological significance and possible therapeutic applications. Pharmacol Rev 50:597–664.

Dingledine R, Borges K, Bowie D, Traynelis SF. 1999. The glutamate receptor ion channels. Pharmacol Rev 51:7–61.

Fukasawa Y, Segawa H, Kim JY, Chairoungdua A, Kim DK, Matsuo H, Cha SH, Endou H, Kanai Y. 2000. Identification and characterization of a Na(+)-independent neutral amino acid transporter that associates with the 4F2 heavy chain and exhibits substrate selectivity for small neutral D- and L-amino acids. J Biol Chem 275: 9690–9698.

Gadea A, López-Colomé AM. 2001. Glial transporters for glutamate, glycine, and GABA III. Glycine transporters. J Neurosci Res 64: 218–222.

Guastella J, Brecha N, Weigman C, Lester HA, Davidson N. 1992. Cloning, expression, and localization of a rat brain high-affinity glycine transporter. Proc Natl Acad Sci USA 89:7189–7193.

Haradahira T, Suzuki K. 1999. An improved synthesis of [^{11}C]L-703,717 as a radioligand for the glycine site of the NMDA receptor. Nucl Med Biol 26:245–247.

Haradahira T, Zhang MR, Okauchi T, Maeda J, Kawabe K, Kida T, Suzuki K, Suhara T. 2000. A strategy for increasing the brain uptake of radioligand in animals: use of a drug that inhibits plasma protein binding. Nucl Med Biol 27:357–360.

Haradahira T, Okauchi T, Maeda J, Zhang MR, Kida T, Kawabe K, Mishina M, Watanabe Y, Suzuki K, Suhara T. 2002. A positron-emitter labeled glycine$_B$ site antagonist, [^{11}C]L-703,717, preferentially binds to a cerebellar NMDA receptor subunit consisting of GluR ε3 subunit in vivo, but not in vitro. Synapse 43:131–133.

Hashimoto A, Nishikawa T, Konno R, Niwa A, Yasumura Y, Oka T, Takahashi K. 1993a. Free D-serine, D-aspartate and D-alanine in central nervous system and serum in mutant mice lacking D-amino acid oxidase. Neurosci Lett 152:33–36.

Hashimoto A, Nishikawa T, Oka T, Takahashi K. 1993b. Endogenous D-serine in rat brain: *N*-methyl-D-aspartate receptor-related distribution and aging. J Neurochem 60:783–786.

Hashimoto A, Oka T, Nishikawa T. 1995. Extracellular concentration of endogenous free D-serine in the rat brain as revealed by in vivo microdialysis. Neuroscience 66:635–643.

Honer M, Benke D, Laube B, Kuhse J, Heckendorn HA, Angust C, Monyer H, Seeburg PH, Betz H, Mohler H. 1998. Differentiation of glycine antagonist sites of *N*-methyl-D-aspartate receptor subtypes: preferential interaction of CGP61594 with NR1/NR2B receptors. J Biol Chem 273:11158–11163.

Jursky F, Nelson N. 1995. Localization of glycine neurotransmitter transporter (GLYT2) reveals correlation with the distribution of glycine receptor. J Neurochem 64:1026–1033.

Konno R, Yasumura Y. 1983. Mouse mutant deficient in D-amino acid oxidase activity. Genetics 103:277–285.

Malandro MS, Kilberg MS. 1996. Molecular biology of mammalian amino acid transporters. Annu Rev Biochem 65:305–336.

Manhas MS, Hoffman WH, Lai B, Bose AK. 1975. Steroids. Part X. A convenient synthesis of alkyl aryl ethers. J Chem Soc Perkin Trans I:461–463.

Matsui T, Sekiguchi M, Hasgimoto A, Tomita U, Nishikawa T, Wada K. 1995. Functional comparison of D-serine and glycine in rodents: the effects on cloned NMDA receptors and the extracellular concentration. J Neurochem 65:454–458,1995.

Mori H, Mishina M. 1995. Structure and function of the NMDA receptor channels. Neuropharmacology 34:1219–1237.

Nakauchi J, Matsuo H, Kim DK, Goto A, Chairoungdua A, Cha SH, Inatomi J, Shiokawa Y, Yamaguchi K, Saito I, Endou H, Kanai Y. 2000. Cloning and characterization of a human brain Na(+)-independent transporter for small neutral amino acids that transports D-serine with high affinity. Neurosci Lett 287:231–235.

Palacín M, Estévez R, Bertran J, Zorzano A. 1998. Molecular biology of mammalian plasma membrane amino acid transporters. Physiol Rev 78:969–1054.

Schell MJ, Molliver ME, Snyder SH. 1995. D-Serine, an endogenous synaptic modulator: localization to astrocytes and glutamate-stimulated release. Proc Natl Acad Sci USA 92:3948–3952.

Schell MJ, Brady Jr RO, Molliver ME, Snyder SH. 1997. D-Serine as a neuromodulator: regional and developmental localization in rat brain glia resemble NMDA receptors. J Neurosci 17:1604–1615.

Supplisson S, Bergman C. 1997. Control of NMDA receptor activation by a glycine transporter co-expressed in Xenopus oocytes. J Neurosci 17:4580–4590.

Utsunomiya-Tate N, Endou H, Kanai Y. 1996. Cloning and functional characterization of a system ASC-like Na^+-dependent neutral amino acid transporter. J Biol Chem 271:14883–14890.

Weimar WR, Neims AH. 1977. The development of D-amino acid oxidase in rat cerebellum. J Neurochem 29:649–656.

Yamakura T, Shimoji K. 1999. Subunit- and site-specific pharmacology of the NMDA receptor channel. Progr Neurobiol 59:279–298.

Yamamoto N, Tomita U, Umino A, Nishikawa T. 2001. Uptake of D-serine by synaptosomal P2 fraction isolated from rat brain. Synapse 42:84–86.

Zafra F, Aragón C, Olivares L, Danbolt NC, Giménez C, Storm-Mathisen J. 1995. Glycine transporters are differentially expressed among CNS cells. J Neurosci 15:3952–3969.

Zhang MR, Haradahira T, Suhara T, Maeda J, Okauchi T, Kida T, Kawabe K, Suzuki K. 2000. Synthesis of GLYT1-selective inhibitor [^{11}C]NFPS. Jpn J Nucl Med 37:570.

ELSEVIER

Nuclear Medicine and Biology 30 (2003) 513–519

NUCLEAR MEDICINE — AND — BIOLOGY

www.elsevier.com/locate/nucmedbio

[^{11}C]DAA1106: Radiosynthesis and *in vivo* binding to peripheral benzodiazepine receptors in mouse brain

Ming-Rong Zhang[a,b,*], Takayo Kida[a,b], Junko Noguchi[a,b], Kenji Furutsuka[a,b], Jun Maeda[a,b], Tetsuya Suhara[a,c], Kazutoshi Suzuki[a]

[a]*Department of Medical Imaging, National Institute of Radiological Sciences, 4-9-1 Anagawa, Inage-ku, Chiba 263-8555, Japan*
[b]*SHI Accelerator Service Co. Ltd., 5-9-11 Kitashinagawa, Shinagawa-ku, Tokyo 141-8686, Japan*
[c]*CREST, Japan Sciences and Technology Corporation, 4-1-8 Honmachi, Kawaguchi 332-0012, Japan*

Received 14 September 2002; received in revised form 24 December 2002; accepted 05 January 2003

Abstract

DAA1106 (*N*-(2,5-Dimethoxybenzyl)-*N*-(5-fluoro-2-phenoxyphenyl)acetamide), is a potent and selective ligand for peripheral benzodiazepine receptors (PBR) in mitochondrial fractions of rat (K_i=0.043 nM) and monkey (K_i=0.188 nM) brains. This compound was labeled by [^{11}C]methylation of a corresponding desmethyl precursor (DAA1123) with [^{11}C]CH_3I in the presence of NaH, with a 72±16% (corrected for decay) incorporation yield of radioactivity. After HPLC purification, [^{11}C]DAA1106 was obtained with ≥98% radiochemical purity and specific activity of 90–156 GBq/μmol at the end of synthesis. After *iv* injection of [^{11}C]DAA1106 into mice, high accumulations of radioactivity were found in the olfactory bulb and cerebellum, the high PBR density regions in the brain. Coinjection of [^{11}C]DAA1106 with unlabeled DAA1106 and PBR-selective PK11195 displayed a significant reduction of radioactivity, suggesting a high specific binding of [^{11}C]DAA1106 to PBR. Although this tracer was rapidly metabolized in the plasma, only [^{11}C]DAA1106 was detected in the brain tissues, suggesting the specific binding in the brain due to the tracer itself. These findings revealed that [^{11}C]DAA1106 is a potential and selective positron emitting radioligand for PBR.

Keywords: peripheral benzodiazepine receptor; PBR; carbon-11; DAA1106; PET

1. Introduction

Benzodiazepine receptors are divided into two types: central and peripheral benzodiazepine receptors. The central benzodiazepine receptor (CBR) is mainly localized on the extracellular domain of the γ-aminobutyric acid (GABA) receptor, and modulates the postsynaptic chloride channel gating by GABA on $GABA_A$ receptor [30]. Thus, a number of ligands for this receptor have been developed as anxiolytics and anticonvulsants [1,31]. On the other hand, the peripheral benzodiazepine receptor (PBR) has distinct pharmaceutical properties from CBR in that it has a low affinity for most benzodiazepines [2,33]. PBR, which was initially identified in the peripheral tissues, is located on the mitochondrial outer membrane in several organs including the kidney, nasal epithelium, lung, heart and endocrine organs such as the adrenal, testis and pituitary gland [2,4,6]. Later studies further demonstrated the presence of this receptor in the central nervous system [25]. It became clear that the density of PBR in the brain regions can equal or exceed the density of CBR in the corresponding regions, and that PBR might mediate physiological responses in the central nervous system [2,12]. Recent studies have shown that density was increased following brain injury, and this increase was used as indication of neuronal damage or loss in several neurodegenerative disorders, such as Alzheimer's disease [10], Huntington's disease [17], Wernicke's encephalopathy [9], multiple sclerosis [3], epilepsy [24] and stroke-induced brain injury [27].

Recent developments of PET (positron emission tomography) radioligands specific for receptors has made it possible to quantitatively evaluate the density and pharmacological action of receptors in the primate brain, in addition to the receptor occupancy of therapeutic drugs, which provide information concerning the most effective doses of drug therapy [11,13]. [^{11}C]]PK11195, a positron emitting radio-labeled compound, was developed as a clinically use-

* Corresponding author: Tel.: 81-43-206-4041; fax: 81-43-206-3261.
E-mail address: zhang@nirs.go.jp (M-R. Zhang).

0969-8051/03/$ – see front matter
doi:10.1016/S0969-8051(03)00016-7

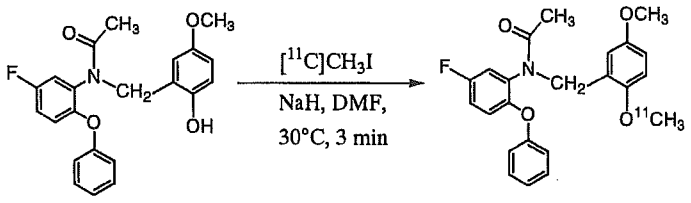

DAA1123 [11C]DAA1106

Fig. 1. Radiosynthesis of [11C]DAA1106.

ful PET tracer for characterizing PBR [7]. However, the relatively low uptake of this tracer into the brain limited its wide application [20,21,24]. The precise characterization for PBR awaits development of new PET tracers with improved behaviors over [11C]]PK11195.

Thus, the aim of this work was to develop a PET tracer that would provide selective imaging of PBR *in vivo*, and to elucidate the pharmacological role of PBR in the central nervous system. Recently, *N*-(2,5-dimethoxybenzyl)-*N*-(5-fluoro-2-phenoxyphenyl)acetamide (DAA1106, Fig. 1) was reported by Taisho Pharmaceutical Co. as a potent and selective ligand for PBR [8,18]. DAA1106 displayed a higher affinity for PBR in mitochondrial fractions of rat (K_i=0.043 nM) and monkey (K_i=0.188 nM) brains than PK11195 [8]. This compound inhibited [3H]PK11195 binding to membranes of rat whole brain (IC_{50}=0.92 nM), whereas it did not inhibit CBR-selective [3H]flunitrazepam (IC_{50}=10,000 nM) [18]. Moreover, DAA1106 showed weak affinities (IC_{50}=10,000 nM) for melanin, $Kappa_1$ and $GABA_A$ receptors, and negligible affinities (IC_{50}>10,000 nM) for 54 others including receptors, ion channels, uptake/transporters and second messengers [18]. To our knowledge, DAA1106 is the most potent and selective ligand for PBR among the compounds previously reported [5,12,26,33]. From the *in vitro* information, DAA1106 appears to be an excellent PET tracer candidate. Moreover, this compound structurally has a methoxy group on the benzene ring and therefore is suitable for labeling with [11C]CH_3I without changing its chemical structure. These observations prompted us to synthesize [11C]DAA1106 and characterize its *in vivo* behavior. In this study, DAA1106 was labeled with 11C by alkylation of the desmethyl precursor DAA1123 with [11C]CH_3I (Fig. 1). The synthetic procedure, purification and formulation are described. The time course, inhibition studies and metabolite analysis of [11C]DAA1106 in mice are reported.

2. Materials and methods

2.1. General

Carbon-11 was produced by $^{14}N(p, \alpha)\ ^{11}C$ nuclear reaction using a CYPRIS HM-18 cyclotron (Sumitomo Heavy Industry Co. Ltd., Tokyo, Japan). A dose calibrator (IGC-3R Curiemeter; Aloka, Tokyo, Japan) was used for all radioactivity measurements if not otherwise stated. Reverse phase high performance liquid chromatography (HPLC) was performed using a JASCO HPLC system: effluent radioactivity was determined using a NaI (Tl) scintillation detector system.

DAA1106 and its desmethyl precursor DAA1123 (*N*-5-fluoro-2-phenoxyphenyl)-*N*-(2-hydroxy-5-methoxybenzyl)-acetamide) were provided by Taisho Pharmaceutical Co. Ltd. (Ohmiya, Japan). PK11195 and Ro15-1788 were purchased from Sigma Co. Ltd. (Milwaukee, WI). DAA1106, PK11195 and Ro15-1788 were dissolved in distilled water and ethanol (1 mg/1.8 mL/0.2 mL) and used for *in vivo* studies. If not otherwise stated, chemicals were purchased from Wako Pure Industries Co. Ltd. (Osaka, Japan) and Aldrich Co. Ltd. (Milwaukee, WI) with the highest grade commercially available. The animal experiment was carried out according to the recommendations of the committee for the care and use of laboratory animals, National Institute of Radiological Sciences (NIRS).

2.2. Radiochemical synthesis

[11C]CH_3I for radiosynthesis was synthesized from cyclotron-produced [11C]CO_2 as described previously [28]. Briefly, the [11C]CO_2 was bubbled into 50 mM $LiAlH_4$ in anhydrous THF (500 μL). After evaporation of the THF, the remaining complexes were treated with 57% HI (300 μL). [11C]CH_3I was transferred under a helium gas flow with heating into a reaction vessel containing anhydrous DMF (300 μL), DAA1123 (0.3–0.5 mg) and NaH (3–5 μL, 0.5 g/20 mL DMF) cooled to −15 – −20°C. After radioactivity reached a plateau, the reaction vessel was warmed to 30°C and kept for 3 min. After adding CH_3CN/H_2O (6/4, 500 μL), the radioactive mixture was applied to a semi-preparative HPLC column. HPLC semi-preparative purification was completed on a YMC J'sphere ODS-H80 column (10 mm ID × 250 mm) using a mobile phase of CH_3CN/H_2O (60/40) at a flow rate of 6.0 mL/min. The retention time (t_R) for [11C]DAA1106 was 9.5 min, whereas that for DAA1123 was 6.7 min. The radioactive fraction corresponding [11C]DAA1106 was collected in a sterile flask containing polysorbate [80] (75 μL) and ethanol (150 μL), evaporated to dryness under vacuum, re-dissolved in 7 mL of sterile

normal saline and passed through a 0.22 μm Millipore filter for analysis and the animal experiments.

2.3. Radiochemical purity and specific activity determinations

Radiochemical purity was assayed by analytical HPLC (column: CAPCELL PAK C_{18}, 4.6 mm ID × 250 mm, UV at 254 nm; mobile phase: CH_3CN/H_2O = 6/4). The t_R for [^{11}C]DAA1106 was 5.8 min at a flow rate of 2.0 mL/min. Confirmation of [^{11}C]DAA1106's identity was achieved by co-injection with the authentic non-radioactive DAA1106. Specific activity of [^{11}C]DAA1106 was determined by comparison of the assayed radioactivity to the mass associated with the carrier UV peak at 254 nm.

2.4. Biodistribution study in mouse

A saline solution of [^{11}C]DAA1106 (average of 8 MBq/200 μL, specific activity: 120 GBq/μmol) was injected into ddy mice (30–40 g, 9 weeks, male) through the tail vein. Five mice for each time point were sacrificed by cervical dislocation at 1, 5, 15, 30 or 60 min postinjection. The whole brain, liver, lung, heart, kidney, adrenal and blood samples were quickly removed. As for the brain, the cerebellum, olfactory bulb, striatum, hippocampus, thalamus, hypothalamus and cerebral cortex were further dissected and weighed. The radioactivity present in the various tissues were measured in a Packard autogamma scintillation counter, and expressed as a percentage of the injected dose per gram of wet tissue (% ID/g). All radioactivity measurements were corrected for decay.

2.5. Blocking studies

To determine *in vivo* specificity and selectivity of [^{11}C]DAA1106 binding to PBR, DAA1106, PK11195 or Ro15-1788 at a dose of 1 mg/kg each, was mixed with [^{11}C]DAA1106 (8 MBq/200 μL; specific activity: 95 GBq/μmol) and injected into ddy mice (n=5), respectively. At designated time points (1, 5, 15, 30 or 60 min), these mice were sacrificed and the whole brains were removed quickly. The brain tissue samples (cerebellum, olfactory bulb, striatum, hippocampus, thalamus, hypothalamus and cerebral cortex) were dissected and treated as described above.

2.6. Metabolite assay in plasma and brain tissue

After intravenous administration of [^{11}C]DAA1106 (70–90 MBq/200 μL) into ddy mice (n=3), these mice were sacrificed by cervical dislocation at 1, 5, 15, 30 or 60 min postinjection. Blood (0.7–1.0 mL) and whole brain samples were removed quickly. The blood sample was centrifuged at 15,000 rpm for 1 min at 4°C to separate plasma, which (250 μL) was collected in a test tube containing CH_3CN (500 μL) and a solution of the authentic unlabeled DAA1106 (1.1 mg/5.0 mL of CH_3CN, 10 μL). After the tube was vortexed for 15 sec and centrifuged at 15,000 rpm for 1 min for deproteinization, the supernatant was collected. The extraction efficiency of radioactivity into the CH_3CN supernatant ranged from 78% to 91% of the total radioactivity in the plasma. On the other hand, the cerebellum and forebrain including the olfactory bulb were dissected from the mouse brain and homogenized together in an ice-cooled CH_3CN/H_2O (1/1, 1.0 mL) solution containing DAA1106. The homogenate was centrifuged at 15,000 rpm for 1 min at 4°C and supernatant was collected. The recovery of radioactivity into the supernatant was 68–87% based on the total radioactivity in the brain homogenate.

An aliquot of the supernatant (100–500 μL) obtained from the plasma or brain homogenate was injected into the HPLC with a highly sensitive positron detector [26] for radioactivity, and analyzed under the same HPLC conditions described above except the mobile phase of CH_3CN/H_2O with a ratio of 1/1. The percent ratio of [^{11}C]DAA1106 (t_R=10.6 min) to the total radioactivity (corrected for decay) on the HPLC chromatogram was calculated as % = (peak area for [^{11}C]DAA1106/total peak area) × 100.

3. Results and Discussion

[^{11}C]DAA1106 was synthesized by *O*-[^{11}C]methylation of the corresponding phenol precursor DAA1123 with [^{11}C]CH_3I in the presence of NaH at 30°C for 3 min (Fig. 1). The radiochemical yield of [^{11}C]DAA1106 was largely dependent on the amount of NaH used for this reaction. When more than two equivalents of NaH relative to DAA1123 were used, an unknown radioactive product (t_R=7.9 min) was observed in the purification HPLC chromatogram in addition to the desired product [^{11}C]DAA1106 (t_R=9.5 min). Limiting the amount of NaH could restrain the formation of the unknown radioactive product. When one equivalent of NaH was used, only [^{11}C]DAA1106 was formed as a reaction product. Using the optimized reaction condition, [^{11}C]DAA1106 was successfully obtained with radioactivity incorporation yields of 72±16% (based on the HPLC chromatogram, n=8). The radiosynthesis, semi-preparative HPLC, and formulation were completed in an average synthesis time of 22 min (n=8). At the end of the syntheses (EOS), 970–1580 GBq of [^{11}C]DAA1106 was obtained as an injection solution of sterile normal saline after 10–15 min proton (14.2 MeV on target) bombardment at a beam current of 15 μA. The final formulated solution was chemically and radiochemically pure (≥98%) as determined by analytic HPLC. The specific activity of [^{11}C]DAA1106 was 90–156 GBq/μmol at EOS.

The radioactivity time course was determined for six specific regions of the mouse after injection of [^{11}C]DAA1106. Table 1 shows the decay corrected percent dose per gram data for all regions. As shown in Table 1, a

Table 1
Distribution (% injected dose/g tissue: mean ± s.d., n = 5) of [^{11}C]DAA1106 in Mice at 1, 5, 15, 30, 60 min Postinjection

Tissue	1 min	5 min	15 min	30 min	60 min
Blood	2.53 ± 0.28	1.65 ± 0.34	2.41 ± 0.42	2.13 ± 0.53	1.43 ± 0.30
Heart	10.45 ± 1.94	11.59 ± 2.36	16.52 ± 3.41	11.54 ± 1.85	7.49 ± 2.01
Liver	1.35 ± 0.41	1.75 ± 0.41	2.10 ± 0.58	1.81 ± 0.67	1.81 ± 0.54
Kidney	12.40 ± 2.35	12.55 ± 2.43	10.01 ± 1.85	9.55 ± 2.81	7.48 ± 1.58
Adrenal	8.15 ± 1.31	7.41 ± 1.28	6.58 ± 1.45	5.31 ± 0.82	5.10 ± 0.98
Lung	90.15 ± 8.15	80.32 ± 9.14	70.84 ± 8.52	48.15 ± 5.10	28.35 ± 2.10
Brain	2.53 ± 0.94	2.81 ± 1.05	3.54 ± 0.98	2.79 ± 0.68	2.12 ± 0.88

high initial concentration of radioactivity (>5% ID/g) was found in the heart, kidney, adrenal and lung. The distribution pattern of uptake was in agreement with the previous *in vitro* findings on the distribution of PBR in the peripheral systems [4,15]. The highest radioactivity of [^{11}C]DAA1106 was found in the lung and this level was higher than that of [^{11}C]PK11195 [16]. The high uptakes in the lung and heart may be related to the mitochondrial contents containing PBR. On the other hand, a high concentration of radioactivity (2.1–3.5% ID/g) was also found in the brain, the target tissue in this study. The values were about 1.5-2 fold higher than those of [^{3}H]PK11195 in the mouse brain at the corresponding times [16]. These results showed that [^{11}C]DAA1106 with a high lipophilicity (LogP = 3.65) [32] can pass through the blood - brain barrier (BBB), a prerequisite for use in PET.

The radioactivity distribution of [^{11}C]DAA1106 in mouse brain is shown in Table 2. As can be seen, [^{11}C]DAA1106 showed a rapid penetration across BBB into all brain regions at 1 min after *iv* administration. The uptakes of [^{11}C]DAA1106 in the olfactory bulb and cerebellum were higher than 2.8% ID/g at 5 min postinjection. The radioactivity accumulated with time in all regions examined, and the concentrations in these regions reached a peak during 15–30 min, and then declined until 60 min postinjection. Among the brain regions examined, the highest uptake of radioactivity (4.2% ID/g at 30 min) was observed in the olfactory bulb, the highest PBR density area in the mouse brain. Following by the olfactory bulb, a high radioactivity level of [^{11}C]DAA1106 (3.5% ID/g at 30 min) was also detected in the cerebellum, whereas a moderate or low uptake was observed in the cerebral cortex, hypothalamus, striatum and hippocampus. The radioactivity of [^{11}C]DAA1106 in the thalamus was the lowest among the brain regions examined. The uptake pattern of radioactivity was consistent not only with [^{3}H]DAA1106 and [^{3}H]PK11195 binding sites in the rat or mouse brain [4,8,14,23], but also with the regional distribution of PBR in the brain [15,19,33].

The *in vivo* selectivity and specificity of [^{11}C]DAA1106 was tested by co-injecting the unlabeled DAA1106, PBR-selective PK11195 and CBR-selective Ro15-1788 at a dose of 1 mg/kg, with [^{11}C]DAA1106, respectively. The results of these blocking studies at 30 min postinjection are presented in Fig. 2. Co-injection with the unlabeled DAA1106 exhibited a statistically significant reduction of radioactivity in the brain regions compared with the control group. The most significant reduced uptake was found in the olfactory bulb (14% of control) and cerebellum (16% of control). Other brain regions (striatum, hippocampus, thalamus, hypothalamus and cerebral cortex) showed a moderate decrease (20–54%) in the percent uptake of [^{11}C]DAA1106. These results revealed a high specific binding of [^{11}C]DAA1106 in all brain regions examined, especially in the olfactory bulb and cerebellum. PBR-selective PK11195 (1 mg/kg) also produced a significant reduction of radioactivity in all brain regions, to an extent similar to that obtained using of the same amount of the non-radioactive DAA1106. The largest decrease in binding occurred in the olfactory bulb (10%) and in the cerebellum (13%) compared with the saline group. In contrast, CBR-selective Ro15-1788 co-injection did not show a clear inhibitory effect on the uptake of [^{11}C]DAA1106 (Fig. 2). In the cerebellum, hypothalamus and thalamus, Ro15-1788 showed a modest

Table 2
Brain Regional Distribution (% injected dose/g tissue: mean ± s.d., n = 5) of [^{11}C]DAA1106 in Mice at 1, 5, 15, 30, 60 min Postinjection

Region	1 min	5 min	15 min	30 min	60 min
Cerebellum	2.61 ± 0.89	2.78 ± 0.38	3.42 ± 0.28	3.52 ± 0.21	1.86 ± 0.19
Olfactory bulb	2.79 ± 0.61	2.88 ± 0.34	3.56 ± 0.55	4.21 ± 0.45	1.97 ± 0.71
Hippocampus	0.53 ± 0.21	0.82 ± 0.30	1.52 ± 0.31	1.70 ± 0.23	0.80 ± 0.25
Striatum	0.81 ± 0.15	1.28 ± 0.39	1.82 ± 0.35	1.81 ± 0.36	1.12 ± 0.25
Cerebral Cortex	1.42 ± 0.26	1.34 ± 0.10	2.35 ± 0.39	2.30 ± 0.68	1.56 ± 0.69
Hypothalamus	1.28 ± 0.18	1.35 ± 0.18	1.45 ± 0.16	1.41 ± 0.31	1.16 ± 0.38
Thalamus	1.03 ± 0.20	1.51 ± 0.35	1.42 ± 0.21	1.23 ± 0.34	1.19 ± 0.29

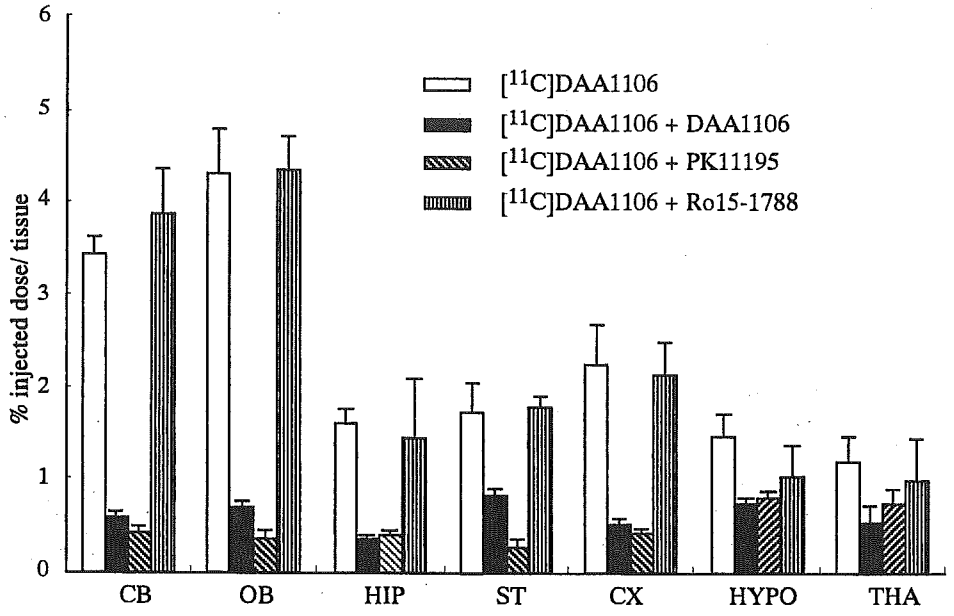

Fig. 2. Effect of unlabeled DAA1106 (1 mg/kg), PBR-selective PK11195 (1 mg/kg) and CBR-selective Ro 15-1788 (1 mg/kg) on [^{11}C]DAA1106 concentrations (mean ± s.d., n=5) in selected regions of mouse brains at 30 min postinjection of [^{11}C]DAA1106 (8 MBq). Abbreviations: CB = cerebellum; OB = olfactory bulb; HIP = hippocampus; ST = striatum; CX = cerebral cortex; HYPO = hypothalamus; THA = thalamus.

(less than 20%) increase in bindings. The cause of the increase can not be presently explained. From these results, it could therefore be suggested that [^{11}C]DAA1106 binds specifically to PBR in the mouse brain *in vivo*. The excellent *in vitro* selectivity of DAA1106 for other neurotransmitters including CBR [8,18] was consistent with this finding.

Metabolites of a radiotracer in the plasma which enter the brain can confound PET imaging studies of neuroreceptors, whether or not the labeled metabolites bind to the target receptor. Therefore, the plasma and extract of homogenized brain tissues of mice were examined by HPLC with a highly sensitive positron detector [29] for radioactivity after *iv* administration of [^{11}C]DAA1106 (70–90 MBq). The percentages of the unchanged [^{11}C]DAA1106 (t_R=10.2 min) in the total radioactivity of the plasma and brain tissues are shown in Fig. 3. As can be seen, in the plasma, the amount of [^{11}C]DAA1106 continued to decrease during the entire experiment and a labeled metabolite was observed as early as 2 min after injection. The fraction corresponding to the unchanged [^{11}C]DAA1106 in the plasma was 65% at 5 min, 17% at 30 min, and 6% of the total radioactivity at 60 min postinjection (Fig. 3). The radiolabeled metabolite was more polar than [^{11}C]DAA1106 as estimated by the retention order (t_R=1.8 min) on a reversed phase HPLC column. In contrast, in the brain homogenate, only [^{11}C]DAA1106 was detected with no evidence (<5%) of any radioactive metabolites even at 60 min postinjection (Fig. 3).

The metabolism of DAA1106 in the rat liver fraction was previously examined and debenzylation of DAA1106 was found to be a major metabolite route [18]. The debenzylated compound (*N*-(5-fluoro-2-phenoxyphenyl)acetamide) was inactive up to 10,000 nM concentration in displacing both [^{3}H]PK11195 from PBR and [^{3}H]flunitrazepam from CBR. Therefore, the presence of this non-radioactive debenzylated metabolite could not affect the specific binding of [^{11}C]DAA1106 in the brain, even if it passed the BBB and entered the brain. On the other hand, no radiolabeled metabolite except the unchanged [^{11}C]DAA1106 was detected in the brain homogenates. Thus, while extensively metabo-

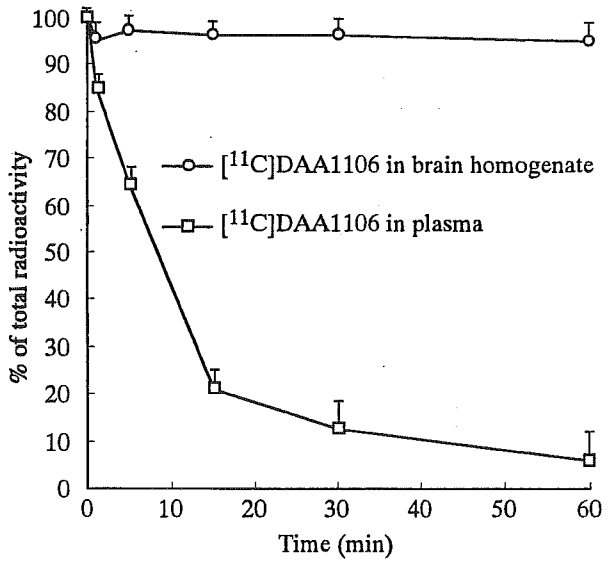

Fig. 3. Percent (mean ± s.d., n=3) of the unchanged [^{11}C]DAA1106 in the plasma and brain homogenate of mouse at several time points after the injection of [^{11}C]DAA1106 (70–90 MBq).

lized in the plasma, the radiolabeled metabolite of [^{11}C]DAA1106 did not appear to cross the BBB in this species. These findings can reveal that all of the specific binding determined in the mouse brain was due to [^{11}C]DAA1106 itself and not influenced by the radiolabeled metabolite.

In conclusion, DAA1106, a potent and selective agonist for PBR in the brain, was successfully labeled with ^{11}C by alkylation of the corresponding desmethyl precursor DAA1123 with [^{11}C]CH_3I with a high incorporation yield of radioactivity. The *in vivo* distribution in mice revealed that [^{11}C]DAA1106 labeled PBR in the mouse brain with high specificity and selectivity. The excellent *in vivo* properties of this radioligand in mice suggested that development for PET imaging in humans should be attractive.

Acknowledgments

The authors are grateful to Drs A. Nakazoto, S. Okuyama and S. Chaki (Taisho Pharmaceutical Co., Ltd.) for giving us samples and helpful suggestions. We are grateful to Mrs T. Igarashi and T. Henmi (Tokyo Nuclear Service Co., Ltd.) for technical support of the radiosynthesis procedures. We also thank the staff of the Cyclotron Operation Section and Radiopharmaceutical Chemistry Section, National Institute of Radiological Sciences (NIRS) for support in the operation of the cyclotron and production of radioisotopes.

References

[1] J.W. Andrews, D.N. Stephents. in: S.E. File (Ed), Psychopharmacology of anxiolytics and antidepressants (1991) pp. 103–130) Pergamon Press: New York.

[2] R.R.H. Anholt, E.B. DeSouza, M.L. Oster-Granite, S.H. Synder, Peripheral-type benzodiazepine receptors: autoradiographic localization in whole-body sections of neonatal rats, J. Pharmac. Exp. Ther. 233 (1985) 517–526.

[3] R. Banati, J. Newcombe, R. Gunn, A. Cagnin, F. Turkheimer, F. Heppner, G. Price, F. Wegner, G. Giovannonni, D. Miller, G. Perkin, T. Smith, A. Hewson, G. Bydder, G. Kreutzber, T. Jones, M. Cuzner, R. Myers, The peripheral-type benzodiazepine binding sites in the brain in multiple sclerosis: Quantitative in vivo imaging of microglia as a measure of disease activity, Brain 123 (2000) 2321–2337.

[4] J. Benavides, D. Quarteronet, F. Imbault, C. Malgouris, A. Uzan, C. Renault, M.C. Dubroeucq, C. Guermy, G. Le Fur, Labelling of "peripheral-type" benzodiazepine binding sites in the rat brain by using [^{3}H]PK11195, an isoquinoline carboxamide derivatives; kinetic studies and autoradiographic localization, J. Neurochem. 41 (1983) 1744–1750.

[5] A. Berson, V. Descatoire, A. Sutton, D. Fau, B. Maulny, N. Vadrot, G. Feldmann, B. Berthon, T. Tordjmann, D. Pessayre, Toxicity of alpidem, a peripheral benzodiazepine receptor ligand, but not zolpidem, in rat hepatocytes: role of mitochondrial permeability transition and metabolic activation, J. Pharmacol. Exp. Ther. 299 (2001) 793–800.

[6] C. Braestrop, R.F. Squires, Specific benzodiazepine receptors in rat brain characterized by high affinity [^{3}H]dizaepam binding, Proc. Natl. Acad. Sci. U.S.A. 74 (1977) 1839–1847.

[7] R. Camsonne, C. Crouzel, D. Comar, M. Maziere, J. Sastre, M.A. Moulin, A. Syrota, Synthesis of N-[^{11}C]-methyl, N-(methyl-1-propyl), (chloro-2-phenyl)-1-isoquinoline carboxamide-3 (PK11195): a new ligand for peripheral benzodiazepine receptors, J. Labelled Comp. Radiopharm. 21 (1984) 985–991.

[8] S. Chaki, T. Funakoshi, R. Yoshikawa, S. Okuyama, T. Okubo, A. Nakazoto, M. Nagamine, K. Tomisawa, Binding characteristics of [^{3}H]DAA1106, a novel and selective ligand for peripheral benzodiazepine receptor, Eur. J. Pharmacolo. 371 (1999) 197–204.

[9] L. Farde, The advantage of using positron emission tomography in drug research, Trends Neurosci 19 (1996) 211–214.

[10] D. Diorio, S. Welner, R. Butterworth, M. Meaney, B. Suranyl-Cadotte, Peripheral benzodiazepine binding sites in Alzheimer's disease frontal cortex and temporal cortex, Neurobiol. Aging 12 (1991) 255–258.

[11] L. Farde, The advantage of using positron emission tomography in drug research, Trends Neurosci. 19 (1996) 211–214.

[12] B. Ferzaz, E. Brault, G. Bourliaud, J.P. Robert, G. Poughon, Y. Claustre, F. Marguet, P. Liere, M. Schumacher, J. Fournier, B. Marabout, M. Sevrin, P. George, J. Benavides, B. Scatton, SR180575 (7-Chloro-*N*, *N*,5-trimethyl-4-oxo-3-phenyl-3,5-dihydro-4*H*-pyridazino[4,5-*b*]indole-1-acetamide), a peripheral benzodiazepine receptor ligand, promotes neuronal survival and repair, J. Pharmacol. Exp. Ther. 301 (2002) 1067–1078.

[13] J.S. Fowler, N.D. Volkow, G.-J., Wang, Y.-S. Ding, S.L. Dewey, PET and drug research and development, J. Nucl. Med. 40 (1999) 1154–1163.

[14] T Funakoshi, S. Chaki, S. Okuyama, T. Okubo, A. Nakazato, M. Nagamine, K. Tomisawa, In vivo receptor labeling of peripheral benzodiazepine receptor by ex vivo binding of [^{3}H]PK11195, Res. Commun. Mol. Pathol. Pharmacol. 105 (1999) 35–41.

[15] M. Gavisg, Y. Katz, S. Bar-Ami, R. Wizman, Biochemical, physiological and pathological aspects of the peripheral benzodiazepine receptor, J. Neurochem. 58 (1992) 1589–1602.

[16] K. Hashimoto, O. Inoue, K. Suzuki, T. Yamasaki, M. Kojima, Synthesis and evaluation of ^{11}C-PK11195 for in vivo study of peripheral-type benzodiazepine receptors using positron emission tomography, Ann. Nucl. Med. 3 (1989) 63–71.

[17] K. Messmer, G. Reynolds, Increased peripheral benzodiazepine binding sites in the brain of patients with Huntington's disease, Neurosci. Lett. 241 (1998) 91–98.

[18] S. Okuyama, S. Chaki, R. Yoshikawa, S. Ogawa, Y. Suzuki, T. Okubo, A. Nakazato, M. Nagamine, K. Tomisawa, Neuropharmacological profile of peripheral benzodiazepine receptor agonists, DAA1097 and DAA1106, Life Sci 64 (1999) 1455–1464.

[19] V. Papadopoulos, H. Amri, H. Li, Z. Yao, R.C. Brown, B. Vidic, M. Culty, Structure, function and regulation of the mitochondrial peripheral-type benzodiazepine receptor, J. Pharmacol. Exp. Ther. 299 (2001) 793–800.

[20] S. Pappata, P. Cornu, Y. Samson, J. Benavides, B. Scatton, C. Crouzel, J.J. Hauw, A. Syrota A, PET study of carbon-11-PK11195 binding to peripheral type benzodiazepine sites in glioblastoma: a case report, J. Nucl. Med. 32 (1991) 1608–1610.

[21] S. Pappata, M. Levasseur, R.N. Gunn, R. Myers, C. Crouzel, A. Syrota, T. Jones, G. W. Kreutzberg, R.B. Banati, Thalamic microglial activation in ischemic stroke detected in vivo by PET and [^{11}C]PK11195, Neurology 55 (2000) 1052–1054.

[22] E. Remeo, J. Auta, A. Kozikowski, D. Ma, V. Papadopoulos, G. Puia, A. Guidotti, 2-Aryl-3-indoleacetamides (FGIN-1): a new class of potent and specific ligand for the mitochondrial DBI receptor (MDR), J. Pharmacol. Exp. Ther. 262 (1992) 971–978.

[23] G.W. Price, R.G. Ahier, S.P. Hume, R. Myers, L. Manjil, J.E. Cremer, S.K. Luthra, C. Pascali, V. Pike V., R.S.J. Frackowiak, In vivo binding to peripheral benzodiazepine binding sites in lesioned rat brain: comparison between [^{3}H]PK11195 and [^{18}F]PK14105 as markers for neuronal damage, J. Neurochem. 55 (1990) 175–185.

[24] A. Sauvageau, P. Desjardins, V. Lozeva, C. Rose, A.S. Hazell, A. Bouthillier, R.F. Butterwort, Increased expression of "peripheral-type" benzodiazepine receptors in human temporal lobe epilepsy: implications for PET imaging of hippocampal sclerosis, Metab. Brain. Dis. 17 (2002) 3–11.

[25] H. Schoemaker, M. Bliss, H.I. Yamamura, Specific high affinity saturable binding to [^{3}H]Ro5-4864 benzodiazepine binding sites in rat cerebral cortex, Eur. J. Pharmacol. 71 (1981) 173–175.

[26] S. Selleri, F. Bruni, C. Costagli, A. Costanzo, G. Guerrini, G. Ciciani, B. Costa, C. Martini, 2-Arylpyrazolo[1,5-a]pyrimidin-3-yl acetamides, New potent and selective peripheral benzodiazepine receptor ligands, Bioorg. Med. Chem. 9 (2001) 2661–2671.

[27] D. Stephenson, D. Scober, E. Smaltig, E. Mincy, D. Gehlert, J. Clements, Peripheral benzodiazepine receptors are colocalized with activated microglia following transient global forbrain ischemia in the rat, J. Nuerosci. 15 (1995) 5263–5274.

[28] K. Suzuki, O. Inoue, K. Hashimoto, T. Yamasaki, M. Kuchiki, K. Tamate, Computer-controlled large scale production of high specific activity [^{11}C]Ro15-1788, Appl. Radiat. Isot. 36 (1985) 971–976.

[29] M. Takei, T. Kida, K. Suzuki, Sensitive measurement of positron emitters eluted from HPLC, Appl. Radiat. Isot. 55 (2001) 229–234.

[30] J.F. Tallman, J.W. Thomas, D.W. Gallager, GABAergic modulation of benzodiazepine binding site sensitivity, Nature 274 (1978) 383–385.

[31] J.F. Tallman, S.M. Paul, P. Skolick, D.W. Gallager, Receptors for the age of anxiety: pharmacology of the benzodiazepine, Science 207 (1980) 274–281.

[32] M.-R. Zhang, A. Tsuchiyama, T. Haradahira, K. Furutsuka, Y. Yoshida, T. Kida, J. Noguchi, T. Irie, K. Suzuki, Procedure for measuring the LogP was according to the article: Synthesis and preliminary evaluation of [^{18}F]FEtP4A, a promising PET tracer for mapping acetylcholinesterase *in vivo*, Nucl. Med. Biol. 29 (2002) 463–468.

[33] D.M. Zisterer, D.C. Williams, Peripheral-type benzodiazepine receptors, Gen. Pharmac. 29 (1997) 305–314.

SYNAPSE 48:184–188 (2003)

No Association Between Genotype of the Promoter Region of Serotonin Transporter Gene and Serotonin Transporter Binding in Human Brain Measured by PET

KUNIHIKO SHIOE,[1] TETSUYA ICHIMIYA,[2,3] TETSUYA SUHARA,[2,3] AKIHIRO TAKANO,[2,3] YASUHIKO SUDO,[2,3] FUMIHIKO YASUNO,[2,3] MASAMI HIRANO,[1] MANABU SHINOHARA,[1] MASATO KAGAMI,[1] YOSHIRO OKUBO,[2,3,4] MASAHIRO NANKAI,[5] AND SHIGENOBU KANBA[1]*

[1]*Department of Neuropsychiatry, Faculty of Medicine, University of Yamanashi, Tamaho, Japan*
[2]*Brain Imaging Project, National Institute of Radiological Sciences, Chiba, Japan*
[3]*CREST, Japan Science and Technology Corporation, Kawaguchi, Japan*
[4]*Biofunctional Informatics, Graduate School of Allied Health Sciences, Tokyo Medical and Dental University, Tokyo, Japan*
[5]*Tokyo Metropolitan Police Hospital, Tokyo, Japan*

KEY WORDS 5-HTTLPR; polymorphism; 5-HTT binding; PET; binding potential

ABSTRACT The human serotonin transporter (5-HTT) gene has a polymorphism in the 5′-flanking promoter region that is called the serotonin transporter gene-linked polymorphic region (5-HTTLPR). In lymphoblast cell lines, the promoter activity of the 5-HTT gene is dependent on 5-HTTLPR allelic variants. The transcriptional activity of the *l* allele was more than twice as high as that of the *s* allele. The *s* allele is considered to be associated with mood disorders and anxiety-related personality traits. To evaluate the functional differences of 5-HTTLPR in the brain in vivo, we examined the allelic variations of 5-HTTLPR and measured 5-HTT binding in the living human brain using positron emission tomography (PET) with C^{11}-labeled trans-1, 2, 4, 5, 6, 10-β-hexahydro-6-[4-(methylthio) phenyl]pyrrolo[2,1-a]isoquinoline (McN5652) as a ligand. Twenty-seven healthy male subjects participated in this study. Although the human lymphoblast cells with the *l/l* genotype was reported to produce higher concentrations of both mRNA and protein of 5-HTT than those with the *l/s* or *s/s* genotype in a human lymphoblast in vitro study, 5-HTT binding in vivo was not significantly different among subjects with the three genotypes (*l/l*: 0.842 ± 0.184, *l/s*: 0.708 ± 0.118, *s/s*: 0.825 ± 0.209). In conclusion, this study does not support the assumption that the genotype-dependent differences of 5-HTTLPR directly contributes to the regulation of the 5-HTT binding site in the living human brain. **Synapse 48:184–188, 2003.**

INTRODUCTION

The serotonin transporter (5-HTT) is the major regulator of serotonergic neurotransmission in the central nervous system (Rudnick and Clark, 1993). 5-HTT has been suggested to play an important role in the pathophysiology of mood disorders and anxiety disorders (Ellis and Salmond, 1994; Lesch and Mossner, 1998; Owens and Nemeroff, 1994) and is the target of antidepressants and antianxiety agents.

The human 5-HTT gene is encoded on chromosome 17q11.1-q12 (Ramamoorthy et al., 1993) and has a polymorphism in the 5′-flanking promoter region that is called the serotonin transporter gene-linked polymorphic region (5-HTTLPR) (Heils et al., 1995). In lymphoblast cell lines containing the promoter sequence (long or short form of 5-HTTLPR), the promoter activity of the 5-HTT gene is dependent on these allelic variants. The transcriptional activity of the long form allele (*l* allele) was more than twice as high as that of the short form allele (*s* allele) (Collier et al., 1996).

Contract grant sponsors: the Ministry of Education, Culture, Sports, and Technology, Japan, the Ministry of Health, Labor, and Welfare, Japan, and the Neuroscience Project of the Institute of Radiological Sciences, Japan.

*Correspondence to: Shigenobu Kanba, Chairman and Professor, Department of Neuropsychiatry, Faculty of Medicine, University of Yamanashi, Tamaho, Nakakoma, Yamanashi 409-3898, Japan.
E-mail: skanba@res.yamanashi-med.ac.jp

Received 25 November 2002; Accepted 18 February 2003

DOI 10.1002/syn.10204

Some genetic studies have reported the association of the *s* allele with mood disorders and anxiety-related personality traits (Collier et al., 1996; Lesch et al., 1996). Many genetic studies have since been carried out, but a collective view has not yet been obtained.

It is therefore important to clarify whether or not functional 5-HTTLPR, as observed in lymphoblast cells in vitro, regulates the number of 5-HTT in the human brain in vivo and then contributes to the pathophysiology of psychiatric conditions. Three studies have addressed this critical question by the use of single photon emission computed tomography (SPECT) with [^{123}I]β-CIT as a radioligand (Heinz et al., 2000; Jacobsen et al., 2000; Willeit et al., 2001). However, the results remained inconclusive. Thus, a positron emission tomography (PET) study with a more selective ligand is still to be performed.

Trans-1, 2, 4, 5, 6, 10-β-hexahydro-6-[4-(methylthio) phenyl]pyrrolo[2,1-a]isoquinoline (McN5652) has been shown to be a good ligand because it is both selective and has high affinity for 5-HTT (Shank et al., 1988; Suehiro et al., 1993a,b). PET studies with C^{11}-labeled (+)McN5652 showed high accumulation in the thalamus and midbrain but low levels in cortical regions and an even lower level in the cerebellum (Parsey et al., 2000; Szabo et al., 1995), in accordance with the results of binding assays in postmortem human brain (Backstrom et al., 1989; Cortes et al., 1988).

In the present study we used [^{11}C](+)McN5652 to evaluate 5-HTT binding in the living human brain and examined the association with an allelic variation of 5-HTTLPR.

MATERIALS AND METHODS

Subjects

In this PET study we recruited 8 male subjects who were known to have both the *l* alleles and 19 male subjects who had the *l* allele (14 subjects with homozygous and 5 with heterozygous genotypes). All subjects resided in the surrounding community, were Japanese, and were unrelated. They were all under the age of 40 years (25.2 ± 5.78 years; mean ± SD). All of the subjects, based on unstructured psychiatric and medical screening interviews, were free of current or past psychiatric disorders and major medical diseases. None had a family history of neuropsychiatric disorder among first-degree relatives. None was receiving any kind of medication. Written informed consent was obtained from all subjects after the purpose and methods of this study had been fully explained. This study was approved by both the Ethics Committee of the University of Yamanashi, Yamanashi, Japan, and the Ethics and Radiation Safety Committee of the National Institute of Radiological Sciences, Chiba, Japan.

Radiochemistry

[^{11}C](+)McN5652 was synthesized by S-methylation of the corresponding des-methyl precursor, which was stabilized by adding a protecting agent for SH groups, dithiothreitol (DTT), into the reaction medium immediately after the demethylation of McN5652 by an automated procedure (Sasaki et al., 1996). Radiochemical purity was higher than 95%.

Image acquisition and analysis

PET scans were performed using a Siemens ECAT47 system (Siemens, Knoxville, TN), which provides 47 slices with 3.375-mm (center-to-center) thickness. The subjects were placed in a supine position with their eyes closed and ears unplugged. To minimize head movement during each scan, head fixation devices (Fixster Instruments, Stockholm, Sweden) with thermoplastic attachments made to fit the individuals were used. A transmission scan for attenuation correction was performed using a ^{68}Ge-^{68}Ga source. Acquisitions were carried out in 2D mode to avoid the influence of scatter outside of the gantry. A bolus of 661.8 ± 117.3 MBq [^{11}C](+)McN5652 with specific radioactivity of 99.5 ± 42.0 GBμ/mmol was injected via the antecubital vein followed by a 20-ml saline flush. Scans were performed for 90 min immediately after the injection.

Magnetic resonance (MR) images of the brain were obtained from all subjects. Three-dimensional T_1-weighted images of 1-mm thickness and a transaxial view were acquired using a 1.5 T Phillips Gyroscan system (Phillips, Best, Netherlands). The scan parameters were TR/TE 19/10 ms, flip angle 30°, matrix 256 × 205, and FOV 256 mm.

All PET scans were reconstructed using a Ramp filter cut-off frequency of 0.5 (FWHM = 6.7 mm). PET images were coregistered to MR images using SPM99 (Wellcome Department of Cognitive Neurology, London, UK). The tissue concentration of radioactivity was obtained from regions of interests (ROIs), which were manually delineated on coregistered MRI/PET images. ROIs were set on the thalamus and cerebellar cortex, since the cortical accumulation of [^{11}C](+)McN5652 was insufficient for the quantification of specific binding (Parsey et al., 2000).

To quantify the specific binding of [^{11}C](+)McN5652, a graphical analysis method using the cerebellum as a reference region was adopted (Logan et al., 1996), since the amount of 5-HTT in the cerebellum is negligible (Backstrom et al., 1989; Cortes et al., 1988). This method allows estimation of the distribution volume ratio (DVR) between target and reference tissue. We used binding potential (BP) as an index of [^{11}C](+)McN5652 binding. BP is estimated by the use of DVR: BP = DVR −1. Although we observed that nonspecific binding of [^{11}C](+)McN5652 was not uniform among regions, BP obtained from the above equation can also be used for the comparison of groups

TABLE 1. Number of subjects, age, and binding potential in three genotype groups

Genotype	n	Age (mean ± SD)	BP (mean ± SD)
l/l	8	28.9 ± 3.23	0.842 ± 0.184
l/s	5	23.4 ± 3.36	0.708 ± 0.118
s/s	14	24.3 ± 7.21	0.825 ± 0.209

BP, binding potential in the thalamus.

(Ikoma et al., 2002). Graphical analysis requires a mean value of k2, the outflow rate constant to the vascular space. We used a mean k2 value of 0.020, which was obtained from graphical analysis with plasma input function in five normal volunteers (Ikoma et al., 2002). Although the k2 value varies with age and gene polymorphism, it has been demonstrated that a 50% change in the k2 value resulted in only a 2% change in DVR (Logan et al., 1996), and thus a fixed value could be used for our subjects. BP was estimated using time points between 40 and 86 min after injection.

Genotyping procedures

Peripheral blood was drawn from the antecubital vein and genomic DNA was extracted from whole blood by QIAamp® DNA Blood Mini Kit (QIAGEN, Hilden, Germany).

Standard polymerase chain reaction (PCR) was performed with a total volume of 30 μl containing 10 ng genomic DNA, 1.5 mM $MgCl_2$, 0.13 mM of each deoxyribonucleotide (75% 7-deaza-2′-deoxyguanosine-5′-triphosphate), 0.23 μM of each primer (sense, 5′-GGCGTTGCCGCTCTGAATTGC, antisense, 5′-GAGGGACTGAGCTGGACAACCAC (Heils et al., 1996)), 5% dimethyl sulfoxide, and 1.25 U Taq DNA polymerase. A denaturation step at 95°C for 5 min was followed by 35 cycles consisting of denaturation at 95°C for 30 sec, annealing at 61°C for 2.5 min, and extension at 72°C for 30 sec, before a final extension step at 72°C for 4 min was carried out. Cycling amplification was performed by standard method using a GenAmp PCR System 9700 (PE Applied Biosystems, Norwalk, CT). The PCR products were separated by 2% agarose gel with ethidium bromide and visualized under UV illumination.

Statistical analysis

The data are expressed as mean ± SD. The statistical significance of difference in BP between groups was analyzed by Student's *t*-test. All probability values were two-tailed and a P-value < 0.05 was considered significant.

RESULTS

Table 1 shows the results of subjects with different genotypes. The age (mean ± SD) of the three groups was 28.9 ± 3.23, 23.4 ± 3.36, and 24.3 ± 7.21 years. BP of the subjects with *l/l*, *l/s*, and *s/s* genotypes was

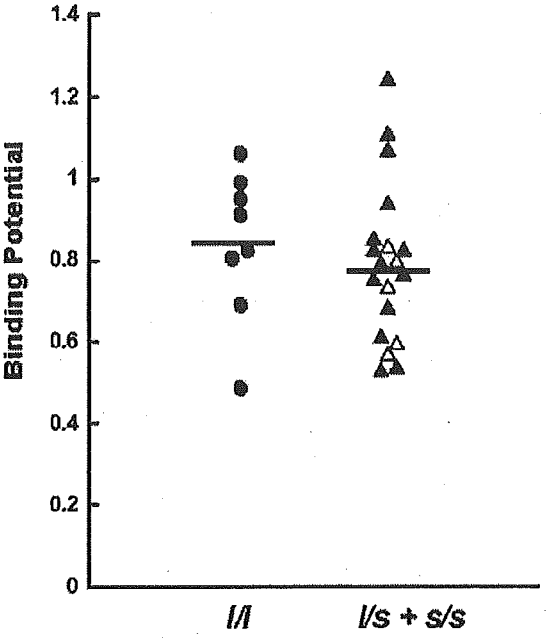

Fig. 1. Genotypes of 5-HTTLPR and binding potential of 5-HTT in the thalamus. There was no significant difference in binding potential between subjects with the *l/l* genotype and those with *l/s* and *s/s* genotypes. Closed circles, subjects with *l/l* genotype; open triangles, subjects with *l/s* genotype; closed triangles, subjects with *s/s* genotype.

0.842 ± 0.184, 0.708 ± 0.118, and 0.825 ± 0.209, respectively.

In an in vitro study (Lesch et al., 1998), the luciferase activity of the transfected *l* form of 5-HTTLPR was more than twice that of the *s* form in human lymphoblast cell lines. Furthermore, human native lymphoblast cells with the genotype *l/l* produced about 1.3–1.7-fold higher levels of mRNA and protein of 5-HTT than cells with the genotype *l/s* or *s/s*. These genotype-dependent differences suggested that the polymorphism has a dominant-recessive effect. Accordingly, we divided the genotypes into two groups (*l/l* and *l/s* + *s/s*; Fig. 1). Nonetheless, the BP values of [^{11}C](+)McN5652 were not significantly different between the groups (0.842 ± 0.184 vs. 0.794 ± 0.194, P = 0.560).

DISCUSSION

The present study shows that the BP values of [^{11}C](+)McN5652 observed in the thalamus of 27 healthy male subjects were fairly constant regardless of the genotype of 5-HTTLPR. Recently, three studies reported a relationship between 5-HTTLPR and 5-HTT binding using SPECT with [^{123}I]β-CIT. Heinz et al. (2000) reported that among eight healthy subjects, *l/l* homozygous individuals had higher 5-HTT availability in the raphe area as compared to *l/s* heterozygous and *s/s* homozygous individuals. On the other hand, using the same methods and analysis, Jacobsen et al. (2000)

reported no effect of 5-HTTLPR on 5-HTT binding in the diencephalon and brain stem of 30 healthy subjects. Willeit et al. (2001) reported that there was no association between an allelic variation of 5-HTTLPR and the in vivo functional regulation of 5-HTT availability in areas of the thalamus-hypothalamus and mesencephalon-pons of 16 healthy subjects.

These SPECT studies used β-CIT, a nonselective monoamine transporter ligand, which has affinity for both 5-HTT and the dopamine transporter, and possibly the norepinephrine transporter (Farde et al., 1994; Little et al., 1993). The pharmacological characteristics of the ligand might have confounded the results obtained by the SPECT studies, since the distribution of each receptor varies depending on the area of the brain examined.

As compared with SPECT using [^{123}I]β-CIT, our PET study using [^{11}C](+)McN5652 has several advantages. First of all, 5-HTT locates densely in the deep structures of the brain such as the thalamus-hypothalamus, basal ganglia, and midbrain-pons. It is generally true that PET provides more accurate measurement of deep brain areas than SPECT, since attenuation correction of those areas with SPECT is generally less accurate than that with PET. We could measure more specific 5-HTT binding by the use of [^{11}C](+)McN5652 (Shank et al., 1988; Suehiro et al., 1993a,b).

In agreement with our results, postmortem studies also did not detect any significant influence of 5-HTTLPR on 5-HTT density in the hippocampus (Naylor et al., 1998) or frontal cortex (Mann et al., 2000). Thus, our study provides further confirmation that there is no association between 5-HTTLPR and 5-HTT binding in vivo in the thalamus.

Recently, other rare allelic variants of 5-HTTLPR have been reported (Kunugi et al., 1997; Nakamura et al., 2000), and some variants showed silencer activity of 5-HTTLPR (Sakai et al., 2002). A further study is necessary to elucidate the more complete picture of the association between the human serotonin transporter linked polymorphic region and 5-HTT binding in the brain.

It is well known that the amount of 5-HTT in the brain is finely regulated by many steps, such as protein folding and insertion into the plasma membrane, and phosphorylation is also speculated to be involved in the control of 5-HTT activity (Blakely et al., 1998). Although [^{11}C](+)McN5652 binding, which might represent the density of 5-HTT, is maintained at the same level, this does not necessarily exclude the possibility that a difference in the regulation of 5-HTT function in the different genotypes may become evident under pathological conditions. In other words, it might be expected that a person with a particular genotype might be more vulnerable to environmental stress and have a higher tendency to develop certain types of psychiatric conditions. To elucidate this possibility, further studies with functional evaluation will be required.

ACKNOWLEDGMENTS

We thank the staff members of the National Institute of Radiological Sciences.

REFERENCES

Backstrom I, Bergstrom M, Marcusson J. 1989. High affinity [^{3}H]paroxetine binding to serotonin uptake sites in human brain tissue. Brain Res 486:261–268.

Blakely RD, Ramamoorthy S, Schroeter S, Qian Y, Apparsundaram S, Galli A, DeFelice LJ. 1998. Regulated phosphorylation and trafficking of antidepressant-sensitive serotonin transporter proteins. Biol Psychiatry 44:169–178.

Collier DA, Stober G, Li T, Heils A, Catalano M, Di Bella D, Arranz MJ, Murray RM, Vallada HP, Bengel D, Muller CR, Roberts GW, Smeraldi E, Kirov G, Sham P, Lesch KP. 1996. A novel functional polymorphism within the promoter of the serotonin transporter gene: possible role in susceptibility to affective disorders. Mol Psychiatry 1:453–460.

Cortes R, Soriano E, Pazos A, Probst A, Palacios JM. 1988. Autoradiography of antidepressant binding sites in the human brain: localization using [^{3}H]imipramine and [^{3}H]paroxetine. Neuroscience 27:473–496.

Ellis PM, Salmond C. 1994. Is platelet imipramine binding reduced in depression? A meta-analysis. Biol Psychiatry 36:292–299.

Farde L, Halldin C, Muller L, Suhara T, Karlsson P, Hall H. 1994. PET study of [^{11}C]β-CIT binding to monoamine transporters in the monkey and human brain. Synapse 16:93–103.

Heils A, Teufel A, Petri S, Seemann M, Bengel D, Balling U, Reiderer P, Lesch KP. 1995. Functional promoter and polyadenylation site mapping of the human serotonin (5-HT) transporter gene. J Neural Trans Gen Sect 102:247–254.

Heils A, Teufel A, Petri S, Stober G, Riederer P, Bengel D, Lesch KP. 1996. Allelic variation of human serotonin transporter gene expression. J Neurochem 66:2621–2624.

Heinz A, Jones DW, Mazzanti C, Goldman D, Ragan P, Hommer D, Linnoila M, Weinberger DR. 2000. A relationship between serotonin transporter genotype and in vivo protein expression and alcohol neurotoxicity. Biol Psychiatry 47:643–649.

Ikoma Y, Suhara T, Toyama H, Ichimiya T, Takano A, Sudo Y, Inoue M, Yasuno F, Suzuki K. 2002. Quantitative analysis for estimating binding potential of brain serotonin transporters with [^{11}C]McN5652. J Cereb Blood Flow Metab 22:490–501.

Jacobsen LK, Staley JK, Zoghbi SS, Seibyl JP, Kosten TR, Innis RB, Gelernter J. 2000. Prediction of dopamine transporter binding availability by genotype: a preliminary report. Am J Psychiatry 157:1700–1703.

Kunugi H, Hattori M, Kato T, Tatsumi M, Sakai T, Sasaki T, Hirose T, Nanko S. 1997. Serotonin transporter gene polymorphisms; ethnic difference and possible association with bipolar affective disorder. Mol Psychiatry 2:457–462.

Lesch KP, Mossner R. 1998. Genetically driven variation in serotonin uptake: is there a link to affective spectrum, neurodevelopmental, and neurodegenerative disorders? Biol Psychiatry 44:179–192

Lesch KP, Bengel D, Heils A, Sabol SZ, Greenberg BD, Petri S, Benjamin J, Muller CR, Hamer DH, Murphy DL. 1996. Association of anxiety-related traits with a polymorphism in the serotonin transporter gene regulatory region. Science 274:1527–1531.

Little KY, Kirkman JA, Carroll FI, Breese GR, Duncan GE. 1993. [^{125}I]RTI-55 binding to cocaine-sensitive dopaminergic and serotonergic uptake sites in the human brain. J Neurochem 61:1996–2006.

Logan J, Fowler JS, Volkow ND, Wang GJ, Ding YS, Alexoff DL. 1996. Distribution volume ratios without blood sampling from graphical analysis of PET data. J Cereb Blood Flow Metab 16:834–840.

Mann JJ, Huang YY, Underwood MD, Kassir SA, Oppenheim S, Kelly TM, Dwork AJ, Arango V. 2000. A serotonin transporter gene promoter polymorphism (5-HTTLPR) and prefrontal cortical binding in major depression and suicide. Arch Gen Psychiatry 57:729–738.

Nakamura M, Ueno S, Sano A, Tanabe H. 2000. The human serotonin transporter gene linked polymorphism (5-HTTLPR) shows ten novel allelic variants. Mol Psychiatry 5:32–38.

Naylor L, Dean B, Pereira A, Mackinnon A, Kouzmenko A, Copolov D. 1998. No association between the serotonin transporter-linked pro-

moter region polymorphism and either schizophrenia or density of the serotonin transporter in human hippocampus. Mol Med 4:671–674.

Owens MJ, Nemeroff CB. 1994. Role of serotonin in the pathophysiology of depression: focus on the serotonin transporter. Clin Chem 40:288–295.

Parsey RV, Kegeles LS, Hwang DR, Simpson N, Abi-Dargham A, Mawlawi O, Slifstein M, Van Heertum RL, Mann JJ, Laruelle M. 2000. In vivo quantification of brain serotonin transporters in humans using [^{11}C]McN 5652. J Nucl Med 41:1465–1477.

Ramamoorthy S, Bauman AL, Moore KR, Han H, Yang-Feng T, Chang AS, Ganapathy V, Blakely RD. 1993. Antidepressant- and cocaine-sensitive human serotonin transporter: molecular cloning, expression, and chromosomal localization. Proc Natl Acad Sci USA 90:2542–2546.

Rudnick G, Clark J. 1993. From synapse to vesicle: the reuptake and storage of biogenic amine neurotransmitters. Biochim Biophys Acta 1144:249–263.

Sakai K, Nakamura M, Ueno S, Sano A, Sakai N, Shirai Y, Saito N. 2002. The silencer activity of the novel human serotonin transporter linked polymorphic regions. Neurosci Lett 327:13–16.

Sasaki M, Suhara T, Kubodera A, Suzuki K. 1996. An improved automated synthesis and in vivo evaluation of PET radioligand for serotonin re-uptake sites: [^{11}C]McN5652X. Jpn J Nucl Med 33: 1319–1327.

Shank RP, Vaught JL, Pelley KA, Setler PE, McComsey DF, Maryanoff BE. 1988. McN-5652: a highly potent inhibitor of serotonin uptake. J Pharmacol Exp Ther 247:1032–1038.

Suehiro M, Scheffel U, Dannals RF, Ravert HT, Ricaurte GA, Wagner HN. 1993a. A PET radiotracer for studying serotonin uptake sites: carbon-11-McN-5652Z. J Nucl Med 34:120–127.

Suehiro M, Scheffel U, Ravert HT, Dannals RF, Wagner HN. 1993b. [^{11}C](+)McN5652 as a radiotracer for imaging serotonin uptake sites with PET. Life Sci 53:883–892.

Szabo Z, Scheffel U, Suehiro M, Dannals RF, Kim SE, Ravert HT, Ricaurte GA, Wagner Jr HN. 1995. Positron emission tomography of 5-HT transporter sites in the baboon brain with [^{11}C]McN5652. J Cereb Blood Flow Metab 15:798–805.

Willeit M, Stastny J, Pirker W, Praschak-Rieder N, Neumeister A, Asenbaum S, Tauscher J, Fuchs K, Sieghart W, Hornik K, Aschauer HN, Brucke T, Kasper S. 2001. No evidence for in vivo regulation of midbrain serotonin transporter availability by serotonin transporter promoter gene polymorphism. Biol Psychiatry 50:8–12.

Original Paper

Cerebrovascular Diseases

Cerebrovasc Dis 2004;18:22–29
DOI: 10.1159/000078604

Received: July 23, 2003
Accepted: January 6, 2004
Published online: May 19, 2004

Long-Term Change in Size of Cerebral Infarction: Predictive Value of Brain Perfusion SPECT Using Statistical Parametric Mapping

Hiroshige Watanabe[a] Yuji Murata[a] Isamu Ohashi[a] Kenji Oda[b]
Eisuke Matsushima[b] Yoshiro Okubo[b] Hitoshi Shibuya[a]

Departments of [a]Radiology and [b]Psychiatry, Faculty of Medicine, Tokyo Medical and Dental University, Tokyo, Japan

Key Words
Brain infarction · Brain ischemia · Brain MR · Single photon emission computed tomography

Abstract
A focus of infarction is surrounded by hypoperfused areas. The present study was undertaken to examine the long-term changes in the size of infarcts, the relationship between the size of an infarct and the extent of the surrounding hypoperfused areas, and the background of such changes. The subjects of this study were 11 patients with ischemic lesions of the brain who had undergone brain SPECT (^{99m}Tc-ethyl cysteinate dimer) within 1 week after initial MRI, and who underwent MRI again more than half a year later. Statistical parametric mapping (SPM) was conducted to detect significantly hypoperfused areas on the SPECT images. Relative size of significantly hypoperfused areas on SPM and infarcts on T_2-weighted MR images were measured. The patients were divided into two groups based on the percentage of the infarct's size relative to the size of the surrounding hypoperfused areas (75–125 and 0–39%). Infarcts in the '75–125%' group showed little change in size, while in the '0–39%' group infarcts increased slowly until it reached the same rate as the former group. All patients with infarct in the '0–39%' group were noted to have severe stenosis of the internal carotid arteries bilaterally. Patients having severe stenosis of the internal carotid artery often had a slowly enlarging infarct. SPM seems to be useful in predicting the ultimate size of the infarct.

Introduction

In regard to the size of cerebral infarcts, it has been reported that many infarcts reach their peak volume within 3 days (more significantly within the first 24–36 h) after the onset, and that their size starts to decrease till the 7th day, to reach their ultimate size [1–3]. It is thought that the most important pathophysiological changes in stroke take place during the first few days after the symptom onset [4].

An infarct is usually surrounded by an area of hypoperfused tissue [5]. The size of the hypoperfused area around an infarct differs from case to case, but the volume of this area is relatively large during the acute stage of infarction, and this area may be deemed as a reversibly ischemic area [6, 7]. It has been suggested that treatment or reperfusion during the acute stage may prevent progression of the extent of infarction and thus improve the prognosis of the patient. Prompted by this suggestion, a number of studies have been conducted, focusing on the acute stage of infarction [8–11].

KARGER
Fax + 41 61 306 12 34
E-Mail karger@karger.ch
www.karger.com

1015–9770/04/0181–0022$21.00/0

Accessible online at:
www.karger.com/ced

Hiroshige Watanabe, MD
Department of Radiology, Faculty of Medicine
Tokyo Medical and Dental University, 5-45, 1-chome, Yushima, Bunkyo-ku
Tokyo 113-8519 (Japan)
Tel. +81 3 5803 5311, Fax +81 3 5803 0147, E-Mail wat@aw.catv.ne.jp